

# Azimuthal Jet Flavor Tomography with CUJET2.0 of Nuclear Collisions at RHIC and LHC

Jiechen Xu

Columbia University

Based on

Jiechen Xu, Alessandro Buzzatti, and Miklos Gyulassy, [arXiv:1402.2956](#), [arXiv:1404.0384](#)

Alessandro Buzzatti, and Miklos Gyulassy, [arXiv:1106.3061](#), [arXiv:1210.6417](#)

For JET Summer School 2014 Student Talk, UC Davis, CA

# Outline

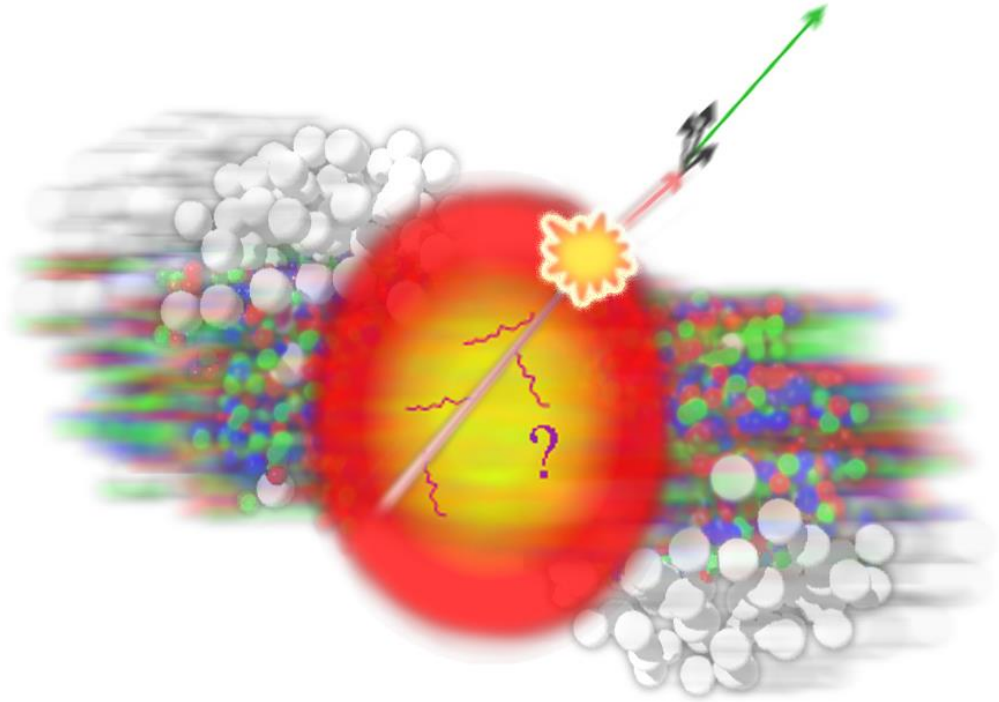
- ❖ Part I: CUJET2.0: A pQCD Model for Azimuthal Jet Flavor Tomography at RHIC and LHC
  - Radiative jet energy loss in QGP: (D)GLV Opacity Expansion
  - Pre-CUJET: WHDG/DGLV, heavy quark puzzle
  - CUJET1.0 = dynamical fixed coupling DGLV + elastic + trans. Glauber & long. Bjorken
  - The surprising transparency of QGP at LHC, multi-scale running strong coupling
  - CUJET2.0 = dynamical running coupling DGLV + elastic + 2+1D viscous hydro
  - CUJET2.0 results on pion/charged hadron RAA and jet transport coefficient
- ❖ Part II: CUJET2.0 Jet Quenching Phenomenology
  - Why light quark and charged hadron RAA at RHIC and LHC are almost the same?
  - Heavy flavor RAA
  - Why pion and beauty RAA have an crossover?
- ❖ Part III: The jet  $v_2$  open problem
  - Puzzle: consistency with (RAA &  $v_2$ ) AND (RHIC & LHC) AND (central & peripheral)
  - CUJET2.0: reaction plane dependent jet quenching pattern
  - CUJET2.0: light flavor  $v_2$
  - CUJET2.0: heavy flavor  $v_2$
- ❖ Summary and Outlook

# Outline

- ❖ Part I: CUJET2.0: A pQCD Model for Azimuthal Jet Flavor Tomography at RHIC and LHC
  - Radiative jet energy loss in QGP: (D)GLV Opacity Expansion
  - Pre-CUJET: WHDG/DGLV, heavy quark puzzle
  - CUJET1.0 = dynamical fixed coupling DGLV + elastic + trans. Glauber & long. Bjorken
  - The surprising transparency of QGP at LHC, multi-scale running strong coupling
  - CUJET2.0 = dynamical running coupling DGLV + elastic + 2+1D viscous hydro
  - CUJET2.0 results on pion/charged hadron RAA and jet transport coefficient
- ❖ Part II: CUJET2.0 Jet Quenching Phenomenology
  - Why light quark and charged hadron RAA at RHIC and LHC are almost the same?
  - Heavy flavor RAA
  - Why pion and beauty RAA have an crossover?
- ❖ Part III: The jet  $v_2$  open problem
  - Puzzle: consistency with (RAA &  $v_2$ ) AND (RHIC & LHC) AND (central & peripheral)
  - CUJET2.0: reaction plane dependent jet quenching pattern
  - CUJET2.0: light flavor  $v_2$
  - CUJET2.0: heavy flavor  $v_2$
- ❖ Summary and Outlook

# *Jet Tomography*

- ❖ Hard processes happen before the formation of the medium
  - Hard parton production in AA collisions can be calculated in the pQCD paradigm
- ❖ Quarks and gluons have final state interaction
  - Parton shower will be modified by interacting with the medium
- ❖ One can use quark or glue jet as a probe, measure the quenching pattern of hadron/lepton jet fragments, and gain information about the QGP evolution profile
  - Or the other way: with a known medium density evolution to study the parton medium interaction mechanism

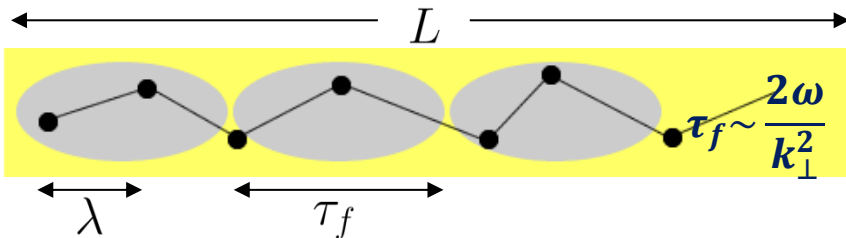


# Radiative Energy Loss

- ❖ Jet quenching models in the pQCD framework based on different underlying assumptions
  - Finite temperature field theory (AMY)
  - Higher twist (HT)
  - Multiple soft scattering (BDMPS-Z and ASW)
  - Opacity expansion (GLV)

## ❖ GLV

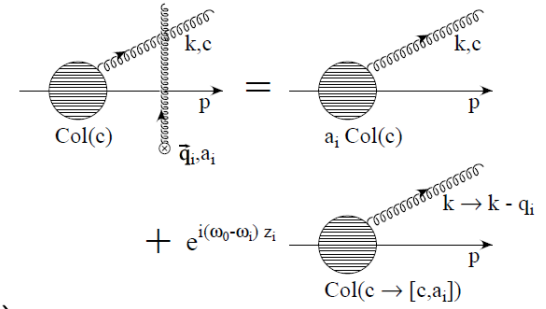
- The plasma is modeled by a series of static or dynamical scattering centers.
- Energy loss is formulated as an expansion in the number of parton-medium scatterings (opacity expansion)
  - ❑ Dominated by the first hard contribution. (“Thin plasma”)
- Include interference of “vacuum” radiation, interference with vertex radiation and interference among subsequent scatterings



- ❑  $\tau_f < \lambda < L$  Incoherent multiple collisions
- ❑  $\lambda < \tau_f < L$  LPM effect
- ❑  $\lambda < L < \tau_f$  “Factorization” limit

# (D)GLV Opacity Expansion

$$\begin{aligned}
 x \frac{dN_g^n}{dx d^2\mathbf{k}} &= \frac{C_R \alpha_s}{\pi^2} \frac{1}{n!} \left( \frac{L}{\lambda_g} \right)^n \int \prod_{i=1}^n (d^2\mathbf{q}_i (|\bar{v}_i(\mathbf{q}_i)|^2 - \delta^2(\mathbf{q}_i))) \\
 &\times -2 \mathbf{C}_{(1\dots n)} \cdot \sum_{m=1}^n \mathbf{B}_{(m+1\dots n)(m\dots n)} \\
 &\times \left( \cos \left( \sum_{k=2}^m \Omega_{(k\dots n)} \Delta z_k \right) - \cos \left( \sum_{k=1}^m \Omega_{(k\dots n)} \Delta z_k \right) \right)
 \end{aligned}$$



$$- \left( -\frac{1}{2} \right)^{N_V} B_i e^{i\omega_0 z_i} [c, a_i] T_{el}$$

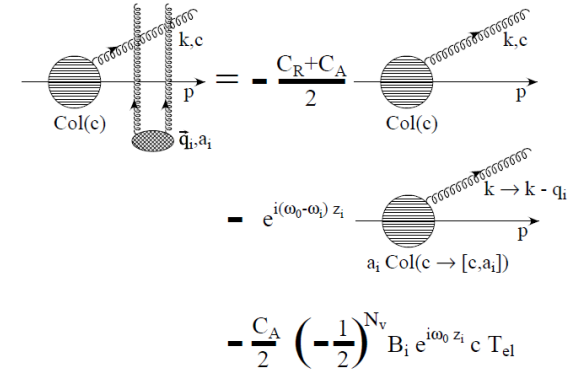
$$\mathbf{C}_{(1\dots n)} = \frac{\mathbf{k} - \mathbf{q}_1 - \dots - \mathbf{q}_n}{(\mathbf{k} - \mathbf{q}_1 - \dots - \mathbf{q}_n)^2 + \chi^2}$$

$$\mathbf{H} = \frac{\mathbf{k}}{\mathbf{k}^2 + \chi^2}$$

$$\mathbf{B}_{(i)} = \mathbf{H} - \mathbf{C}_{(i)}$$

$$\mathbf{B}_{(1\dots m)(1\dots n)} = \mathbf{C}_{(1\dots m)} - \mathbf{C}_{(1\dots n)}$$

$$\Omega_{m\dots n} = \frac{(\mathbf{k} - \mathbf{q}_m - \dots - \mathbf{q}_n)^2 + \chi^2}{2xE}$$



$$- \frac{C_A}{2} \left( -\frac{1}{2} \right)^{N_V} B_i e^{i\omega_0 z_i} c T_{el}$$

$$\chi^2 = M^2 x^2 + m_g^2 (1 - x)$$

$$m_g = \mu / \sqrt{2}, \quad \mu = gT \sqrt{N_c/3 + N_f/6}$$

$$|\bar{v}_i(\mathbf{q}_i)|^2 = \frac{\mu_i^2}{\pi(\mathbf{q}_i^2 + \mu_i^2)^2}$$

# WHDG/DGLV

## Path length fluctuations

$$L(\vec{x}_\perp, \phi) = \int d\tau \rho_p(\vec{x}_\perp + \tau \hat{n}(\phi)) / \langle \rho_p \rangle$$

$$P(E_i \rightarrow E_i - \Delta_{rad} - \Delta_{el}) = \int \frac{d\phi}{2\pi} \int \frac{d^2 \vec{x}_\perp}{N_{bin}(b)} T_{AA}(\vec{x}_\perp, \vec{b}) \otimes P_{rad}(\Delta_{rad}; L(\vec{x}_\perp, \phi)) \otimes P_{el}(\Delta_{el}; L(\vec{x}_\perp, \phi)).$$

## Collisional energy loss

$$\frac{dE^{el}}{dx} = C_R \pi \alpha_s^2 T^2 \left(1 + \frac{n_f}{6}\right) f(v) \log(B_c)$$

$$f(v) = \frac{1}{v^2} \left( v + \frac{1}{2}(v^2 - 1) \log\left(\frac{1+v}{1-v}\right) \right) \xrightarrow{v \rightarrow 1} 1$$

$$B_{Bj} = (4E_p T) / (\mu^2)$$

$$B_{TG} = \left( \frac{4pT}{(E_p - p + 4T)} \right) / (\mu)$$

$$B_{BT} = \begin{cases} \left( 2^{\frac{n_f}{6+n_f}} 0.85 E_p T \right) / \left( \frac{\mu^2}{3} \right) & E_p \gg \frac{M^2}{T} \\ \left( 4^{\frac{n_f}{6+n_f}} 0.36 \frac{(E_p T)^2}{M^2} \right) / \left( \frac{\mu^2}{3} \right) & E_p \ll \frac{M^2}{T} \end{cases}$$

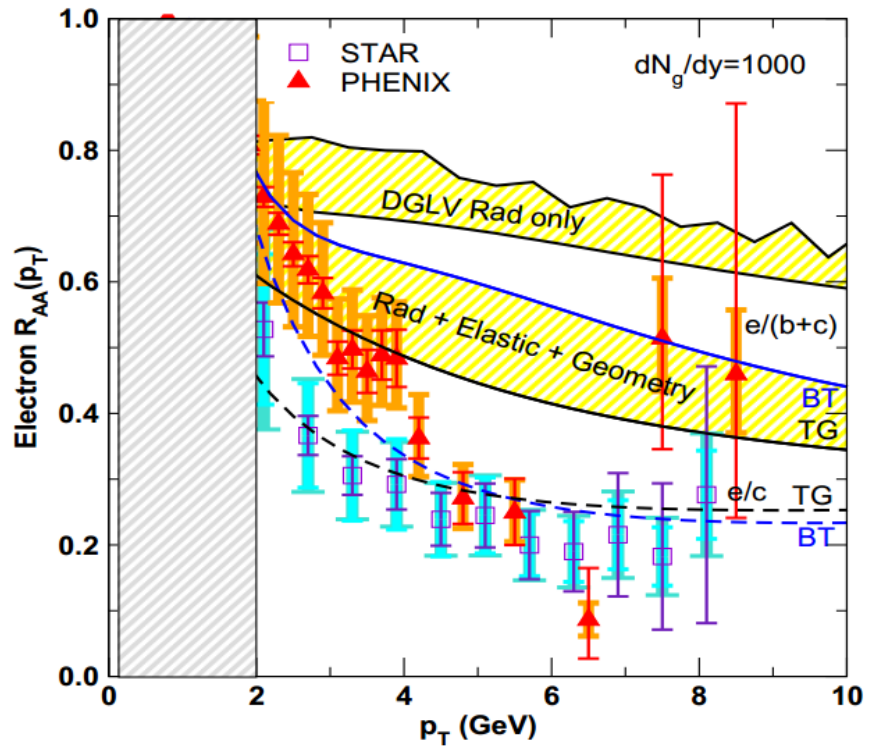
## Convolutions over radiative and elastic

$$P_Q^I(\epsilon; L) = \int dx P_{Q,rad}(x; L) P_{Q,el}(\epsilon - x; L)$$

## Power law assumption of heavy quark pQCD spectra

$$Ed^3\sigma_Q/d^3k \propto 1/p_T^{n+2}$$

$$R_Q^I = \int \frac{d\phi}{2\pi} \int \frac{d^2 \vec{x}_\perp}{N_{bin}(b)} T_{AA}(\vec{x}_\perp, \vec{b}) \int d\epsilon (1 - \epsilon)^n P_Q^I(\epsilon; L(\vec{x}_\perp, \phi)),$$



WHDG, NPA784,426(2007)

❖ "Heavy Quark Puzzle"

**CUJET1.0 = dynamical DGLV + elastic + trans. Glauber + long. Bjorken**

Path length fluctuations

~~$$L(\vec{x}_\perp, \phi) = \int d\tau \rho_p(\vec{x}_\perp + \tau \vec{n}(\phi)) / \langle \rho_p \rangle$$~~

$$P(E_i \rightarrow E_i - \Delta_{rad} - \Delta_{el}) = \int \frac{d\phi}{2\pi} \int \frac{d^2 \vec{x}_\perp}{N_{bin}(\vec{b})} T_{AA}(\vec{x}_\perp, \vec{b}) \otimes P_{rad}(\Delta_{rad}; L(\vec{x}_\perp, \phi)) \otimes P_{el}(\Delta_{el}; L(\vec{x}_\perp, \phi)).$$



$$T(\mathbf{z})|_{\tau MAX} = T_f$$

Radiative energy loss fluctuations

$$P_{rad}(\epsilon) = P_0 \delta(\epsilon) + \tilde{P}(\epsilon)|_0^{\epsilon_{MAX}} + P_1 \delta(\epsilon_{MAX} - \epsilon)$$

Elastic energy loss fluctuations

$$P_{el}(\epsilon) = e^{-\bar{N}_c} \delta(\epsilon) + \mathcal{N} e^{-\frac{(\epsilon - \bar{\epsilon})^2}{4T\bar{\epsilon}/E}}$$

Fragmentation

$$\frac{d\sigma^h}{dp}(p) = \sum_i \int_{p/p_{max}}^1 dx \frac{d\sigma^i}{dp}\left(\frac{p}{x}\right) D^{i \rightarrow h}\left(x; \frac{p}{x}\right)$$

Power law assumption of heavy quark pQCD spectra

~~$$E d^3 \sigma_Q / d^3 k \propto 1/p_T^{n+2}$$~~

~~$$R_Q^I = \int \frac{d\phi}{2\pi} \int \frac{d^2 \vec{x}_\perp}{N_{bin}(\vec{b})} T_{AA}(\vec{x}_\perp, \vec{b}) \int d\epsilon (1 - \epsilon)^n P_Q^I(\epsilon; L(\vec{x}_\perp, \phi)),$$~~



$$\frac{d\sigma^{pp \rightarrow q}}{dp_f d\phi}(p_f; \mathbf{x}_0, \phi) = \int_{p_i^{min}}^{p_i^{max}} dp_i P(p_f, p_i; \mathbf{x}_0, \phi) \frac{d\sigma^{pp \rightarrow q}}{dp_i}(p_i)$$

$$\frac{d\sigma^{AA \rightarrow q}}{dp_f d\phi}(p_f; \phi) = \int d\mathbf{x}_0 \rho_{binary}(\mathbf{x}_0) \frac{d\sigma^{pp \rightarrow q}}{dp_f d\phi}(p_f; \mathbf{x}_0, \phi)$$

ASSUME Poisson distribution for the number of INCOHERENTLY emitted gluons

Gaussian fluctuation for multiple collisions



# Effective Potential

## Static QCD medium (DGLV)

$$|\bar{v}_i(q_i)|^2 = \frac{1}{\pi} \frac{\mu(z_i)^2}{(q^2 + \mu(z_i)^2)^2}$$

- ❖ Static scattering centers
- ❖ Color-electric screened Yukawa potential (Debye mass)
- ❖ Full opacity series

## Dynamical QCD medium (Djordjevic; Gelis; Zakharov)

$$|\bar{v}_i(q_i)|^2 = \frac{1}{\pi} \frac{\mu(z_i)^2}{q^2(q^2 + \mu(z_i)^2)}$$

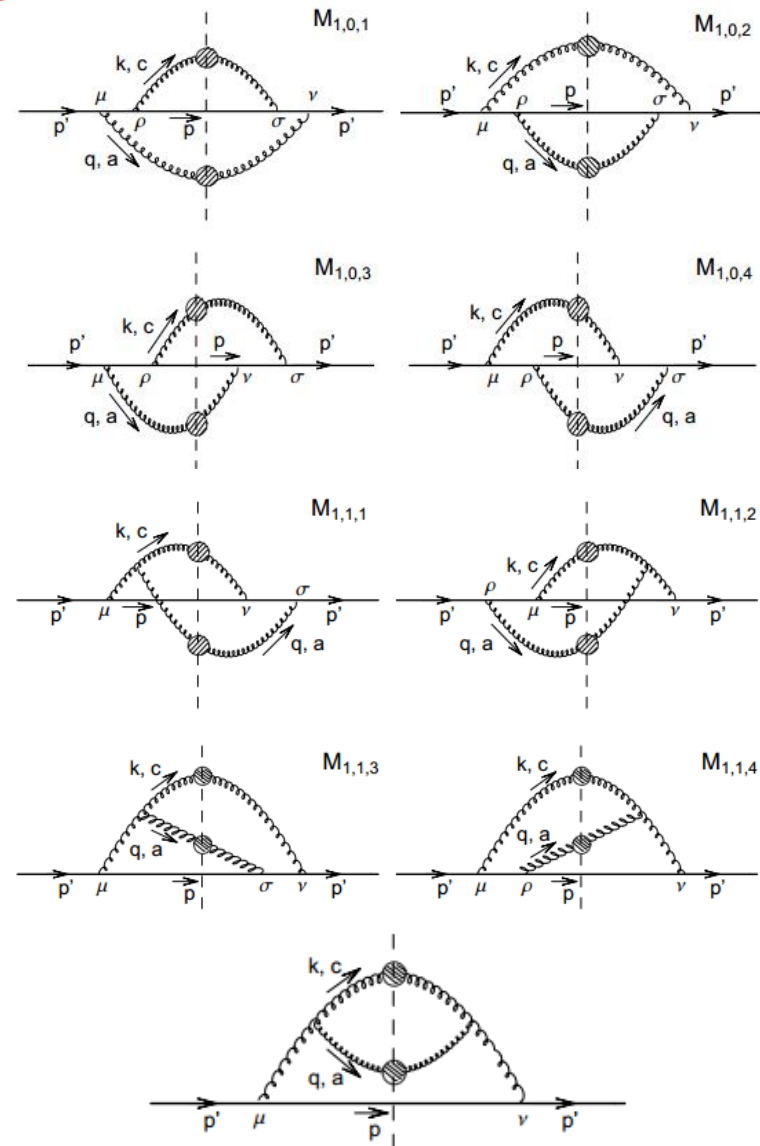
- ❖ Dynamical scattering centers
- ❖ Includes color-magnetic effects (1-HTL gluon propagators)
- ❖ Only first order in opacity

## Interpolating potential (CUJET)

$$|\bar{v}_i(q_i)|^2 = \frac{\mathcal{N}(\mu_e, \mu_m)}{\pi} \frac{\mu_e(z_i)^2 - \mu_m(z_i)^2}{(q^2 + \mu_e(z_i)^2)(q^2 + \mu_m(z_i)^2)}$$

$\mu_e = f_E \mu$        $\mu_m = f_M \mu$

- ❖ Introduces effective color-magnetic screening mass
- ❖ Add  $f_E$  and  $f_M$  allows one to interpolate between the static and dynamical limits, and further explore Non-HTL regime
- ❖ Magnetic screening allows full opacity series



$$\lambda_{\text{dyn}} \iff \lambda_{\text{stat}} = \frac{\lambda_{\text{dyn}}}{c(n_f)} \left[ \frac{\mu^2}{q^2(q^2 + \mu^2)} \right]_{\text{dyn}} \iff \left[ \frac{\mu^2}{(q^2 + \mu^2)^2} \right]_{\text{stat}}$$

## Radiative: dynamical DGLV

$$\begin{aligned}
 x_E \frac{dN_g^{n=1}}{dx_E}(\mathbf{x}_0, \phi) &= \frac{18C_R \alpha_s}{\pi^2} \frac{4 + n_f}{16 + 9n_f} \int d\tau \rho(\mathbf{z}) \int d^2\mathbf{k} \int d^2\mathbf{q} \alpha_s^2 |\tilde{v}(\mathbf{q}, \mathbf{z})|^2 \\
 &\times \frac{-2(\mathbf{k} - \mathbf{q})}{(\mathbf{k} - \mathbf{q})^2 + \chi^2(\mathbf{z})} \left( \frac{\mathbf{k}}{\mathbf{k}^2 + \chi^2(\mathbf{z})} - \frac{(\mathbf{k} - \mathbf{q})}{(\mathbf{k} - \mathbf{q})^2 + \chi^2(\mathbf{z})} \right) \\
 &\times \left( 1 - \cos \left( \frac{(\mathbf{k} - \mathbf{q})^2 + \chi^2(\mathbf{z})}{2x_+ E} \tau \right) \right) \\
 &\times \left( \frac{x_E}{x_+} \right) J(x_+(x_E))
 \end{aligned}$$

$$|\tilde{v}(\mathbf{q}, \mathbf{z})|^2 = \frac{f_E^2 - f_M^2}{(\mathbf{q}^2 + f_E^2 \mu^2(\mathbf{z}))(\mathbf{q}^2 + f_M^2 \mu^2(\mathbf{z}))}$$

$$\chi^2(\mathbf{z}) = M^2 x_+^2 + m_g^2(\mathbf{z})(1 - x_+), \quad m_g(\mathbf{z}) = \mu(\mathbf{z})/\sqrt{2}$$

$$\mu^2(\mathbf{z}) = g^2 f_E^2 T(\mathbf{z})^2 (1 + n_f/6) = 4\pi \alpha_s f_E^2 T(\mathbf{z})^2 (1 + n_f/6)$$

$$0 \leq k_\perp \leq x_E E, \quad 0 \leq q_\perp \leq \text{Min}\{k_\perp, \sqrt{4ET(\mathbf{z})}\}$$

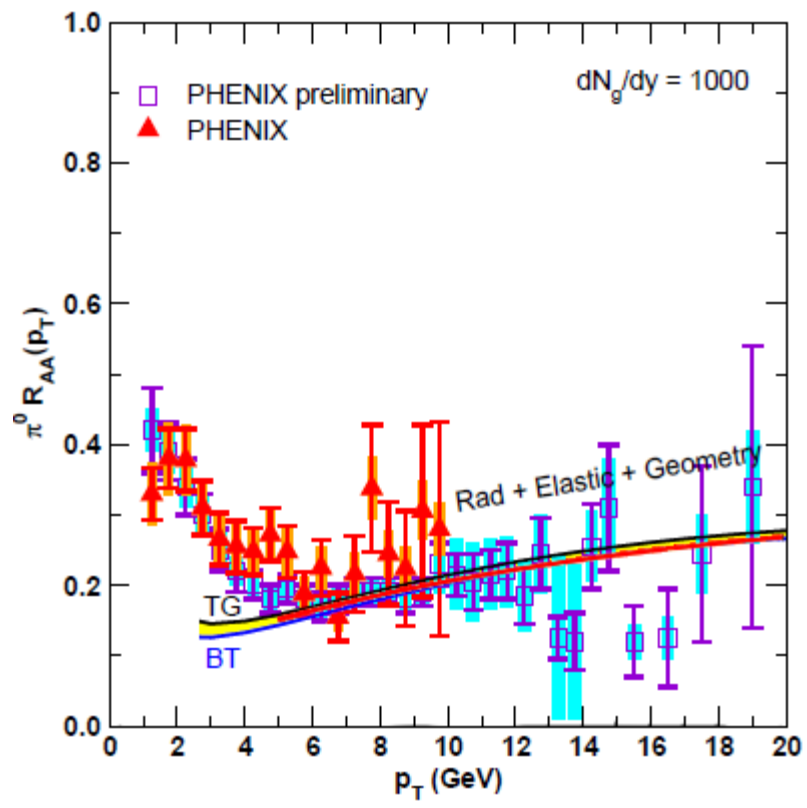
$$x_+(x_E) = \frac{1}{2} x_E \left( 1 + \sqrt{1 - \left( \frac{k_\perp}{x_E E} \right)^2} \right) \quad J(x_+(x_E)) \equiv \frac{dx_+}{dx_E} = \frac{1}{2} \left( 1 + \left( 1 - \left( \frac{k_\perp}{x_E E} \right)^2 \right)^{-1} \right)$$

## Elastic: Thoma-Gyulassy (TG)

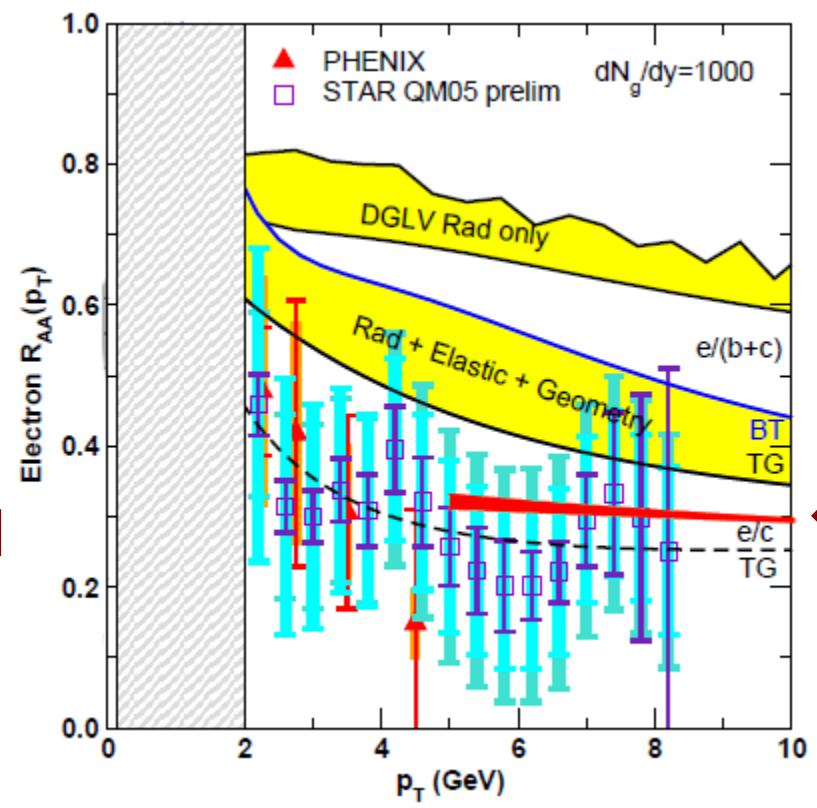
$$\frac{dE(\mathbf{z})}{d\tau} = -C_R \pi \alpha_s^2 T(\mathbf{z})^2 \left( 1 + \frac{n_f}{6} \right) \log \left( \frac{4T(\mathbf{z}) \sqrt{E(\mathbf{z})^2 - M^2}}{\left( E(\mathbf{z}) - \sqrt{E(\mathbf{z})^2 - M^2} + 4T(\mathbf{z}) \right) \mu(\mathbf{z})} \right)$$

# CUJET1.0: To solve heavy quark puzzle

Light Quarks



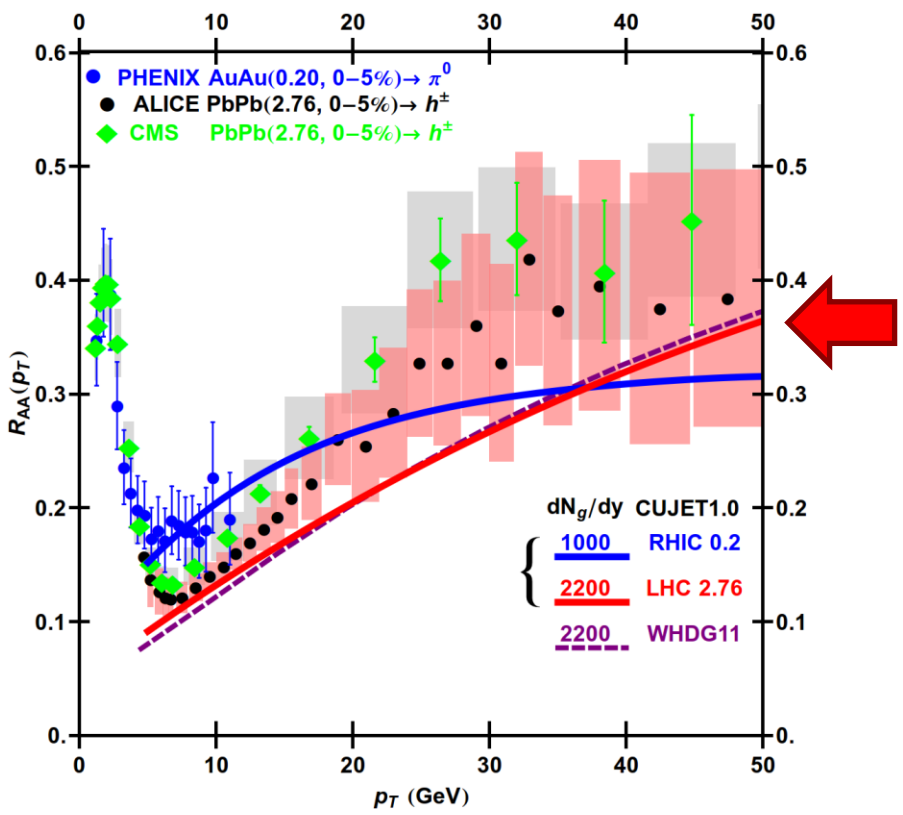
Heavy Quarks



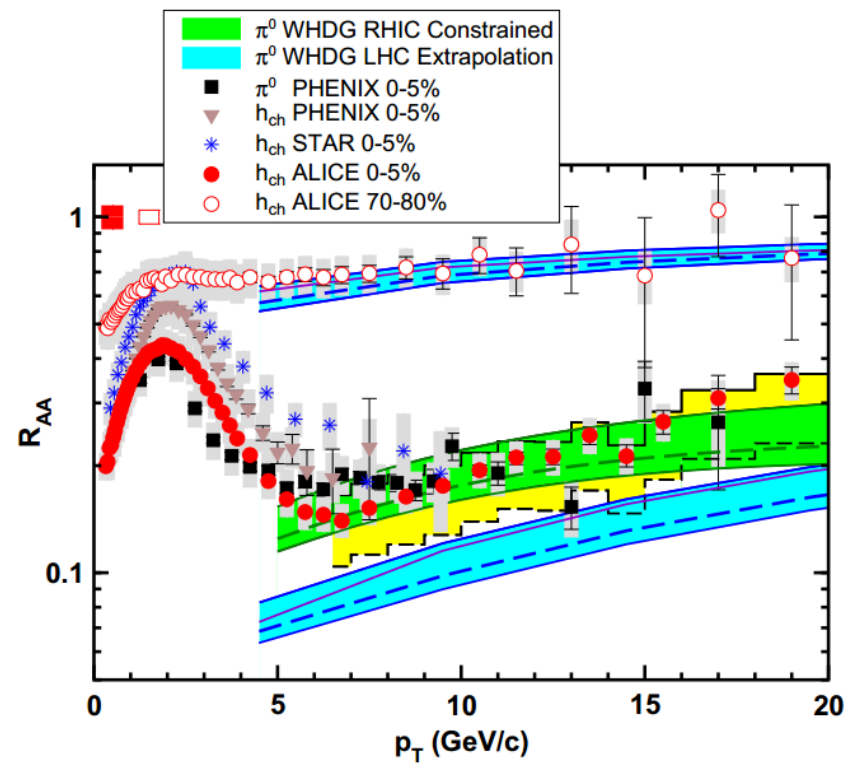
Wicks, Horowitz, Djordjevic, Gyulassy, NPA (2007)

- ❖ Combining dynamical DGLV opacity series and TG elastic energy loss, taking into account more realistic path length fluctuation and convolute over initial production spectra without simplification, CUJET1.0 explains the non-photonic electron  $R_{AA}$  at RHIC

# CUJET1.0: The surprising transparency at LHC



Buzzatti and Gyulassy, PRL108,022301(2012)



Horowitz and Gyulassy, NPA872,265(2011)

- ❖ The CUJET1.0 complication did not explain the surprising transparency of sQGP at LHC
- ❖ Extended  $p_T$  range probed at LHC  $\rightarrow$  Introduce **running coupling** (phenomenologically motivated, rigorous NLO calculation is what to be done)

# Recall fixed coupling CUJET1.0 at first order in opacity

## Radiative: dynamical DGLV

$$\begin{aligned}
 x_E \frac{dN_g^{n=1}}{dx_E}(\mathbf{x}_0, \phi) &= \frac{18C_R \alpha_s}{\pi^2} \frac{4 + n_f}{16 + 9n_f} \int d\tau \rho(\mathbf{z}) \int d^2\mathbf{k} \int d^2\mathbf{q} \alpha_s^2 |\tilde{v}(\mathbf{q}, \mathbf{z})|^2 \\
 &\times \frac{-2(\mathbf{k} - \mathbf{q})}{(\mathbf{k} - \mathbf{q})^2 + \chi^2(\mathbf{z})} \left( \frac{\mathbf{k}}{\mathbf{k}^2 + \chi^2(\mathbf{z})} - \frac{(\mathbf{k} - \mathbf{q})}{(\mathbf{k} - \mathbf{q})^2 + \chi^2(\mathbf{z})} \right) \\
 &\times \left( 1 - \cos \left( \frac{(\mathbf{k} - \mathbf{q})^2 + \chi^2(\mathbf{z})}{2x_+ E} \tau \right) \right) \\
 &\times \left( \frac{x_E}{x_+} \right) J(x_+(x_E))
 \end{aligned}$$

$$|\tilde{v}(\mathbf{q}, \mathbf{z})|^2 = \frac{f_E^2 - f_M^2}{(\mathbf{q}^2 + f_E^2 \mu^2(\mathbf{z}))(\mathbf{q}^2 + f_M^2 \mu^2(\mathbf{z}))}$$

$$\chi^2(\mathbf{z}) = M^2 x_+^2 + m_g^2(\mathbf{z})(1 - x_+), \quad m_g(\mathbf{z}) = \mu(\mathbf{z})/\sqrt{2}$$

$$\mu^2(\mathbf{z}) = g^2 f_E^2 T(\mathbf{z})^2 (1 + n_f/6) = 4\pi \alpha_s f_E^2 T(\mathbf{z})^2 (1 + n_f/6)$$

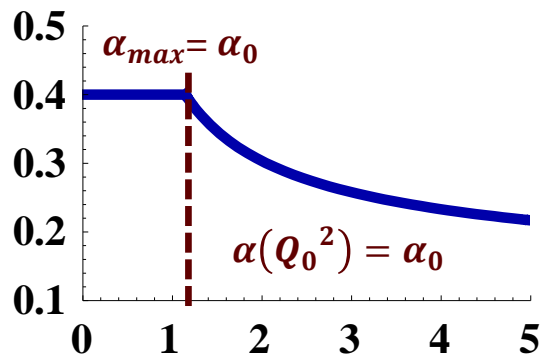
## Elastic: Thoma-Gyulassy (TG)

$$\frac{dE(\mathbf{z})}{d\tau} = -C_R \pi \alpha_s^2 T(\mathbf{z})^2 \left( 1 + \frac{n_f}{6} \right) \log \left( \frac{4T(\mathbf{z}) \sqrt{E(\mathbf{z})^2 - M^2}}{\left( E(\mathbf{z}) - \sqrt{E(\mathbf{z})^2 - M^2} + 4T(\mathbf{z}) \right) \mu(\mathbf{z})} \right)$$

# Multi-scale Running Coupling: Radiative

❖ Introduce one-loop running strong coupling

$$\alpha_s \longrightarrow \alpha_s(Q^2) = \begin{cases} \alpha_0 & \text{if } Q \leq Q_0 \\ \frac{2\pi}{9 \log(Q/\Lambda_{QCD})} & \text{if } Q > Q_0 \end{cases}$$



B. G. Zakharov, JETP Lett. 88 (2008) 781-786

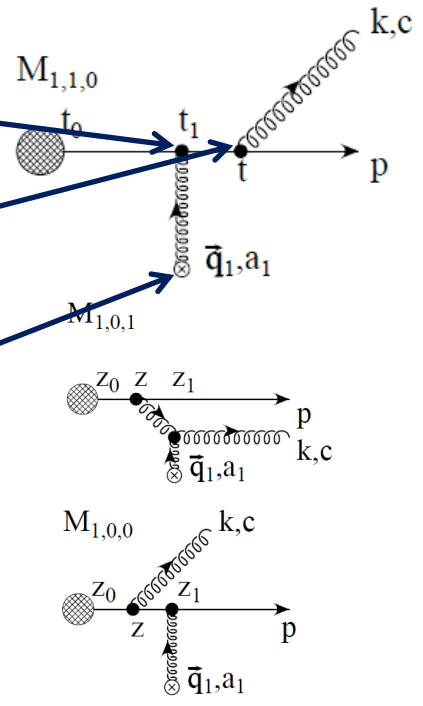
➤ Two powers of  $\alpha_s(Q^2)$  originate from the jet-medium interaction vertices; the exchanged transverse momentum is  $\mathbf{q}$ , and  $Q^2 = \mathbf{q}^2$

➤ One power  $\alpha(Q^2)$  originates from the radiated gluon vertex; the off-shellness of the intermediate quark propagator in the amplitude where the gluon is emitted after the scattering is

$$Q_2^2 = q^2 - M^2 = \frac{\mathbf{k}^2}{x_+(1-x_+)} + \frac{x_+ M^2}{1-x_+} + \frac{m_g^2}{x_+}$$

➤ An ambiguity arises from other amplitudes for example if the radiated gluon scatters with  $q$  instead of the quark. In eikonal limit, assuming mass effects are negligible, keep only  $k$  perp term

➤ One power of the thermal coupling originates from the Debye mass  $m_D(\alpha(Q^2), T)$ ; the scale is set to be proportional to the temperature of the plasma,  $Q^2 = (2T)^2$



# Multi-scale Running Coupling: Elastic

- ❖ S. Peigne and A. Peshier, PRD 77, 114017 (2008)
- ❖ In the limit of  $E \gg k$  (the momentum of target particle in the medium), approximate parton-parton elastic cross section as

$$\frac{d\sigma_{i,j}}{d\hat{t}} = \frac{2\pi\alpha^2}{\hat{t}^2} c_{i,j}$$

- ❖ Energy loss per unit length

$$\frac{dE}{dx} = \int d^3k \rho_i(k) \Phi \int_{\hat{t}_{MIN}}^{\hat{t}_{MAX}} d\hat{t} \frac{d\sigma_{i,j}}{d\hat{t}} \cdot (E - E') \left\{ \begin{array}{l} E - E' = -\frac{\hat{t}}{2k(1 - \cos\theta)} \\ \Phi = 1 - \cos\theta \end{array} \right.$$



$$\frac{dE}{dx} = -\pi C_R \frac{\alpha^2}{\beta^2} \left(1 + \frac{n_f}{6}\right) \log B \longleftrightarrow \frac{dE}{dx} = \frac{4\pi}{3} C_F \alpha_s^2 T^2 \left(\frac{1}{v} + \frac{v^2 - 1}{2v^2} \log \frac{1+v}{1-v}\right) \log \left(\frac{k_{max}}{\mu_D}\right)$$

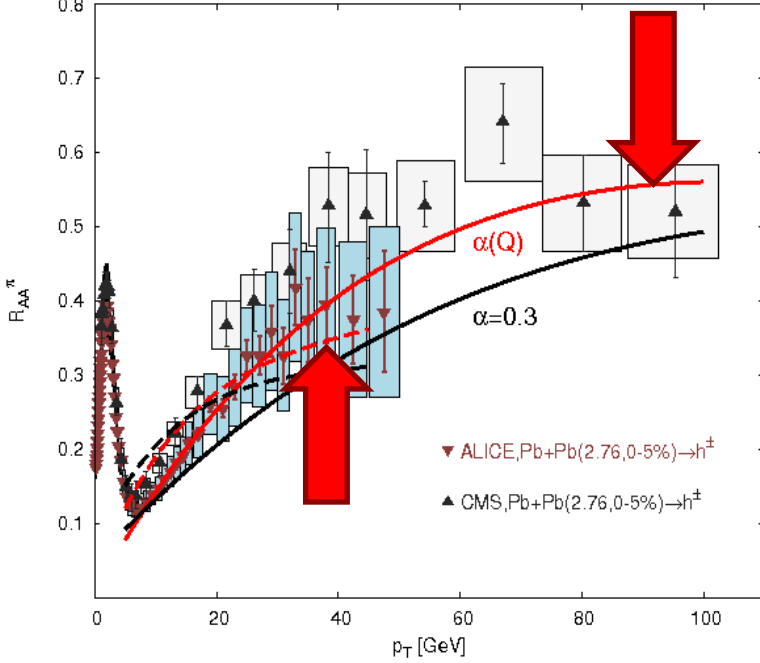
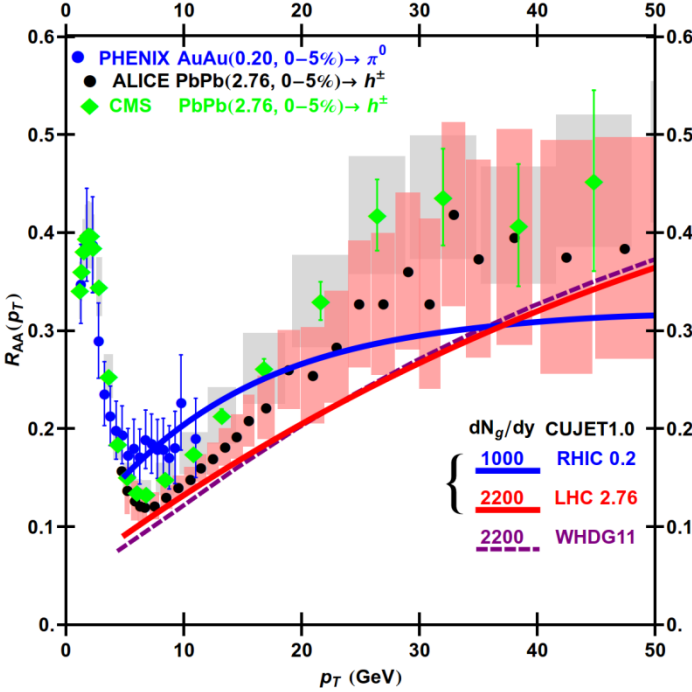
$$\alpha_s^2 \int_{\mu^2}^{4ET} \frac{d\hat{t}}{\hat{t}} \longrightarrow \int_{\mu^2}^{4ET} \frac{d\hat{t}}{\hat{t}} \alpha_s^2(\hat{t})$$

$$\alpha_s(|t|) = [4\pi\beta_0 \ln(|t|/\Lambda^2)]^{-1}$$

$$q_{\perp}^{MAX} = \sqrt{4ET}$$

$$\alpha_s^2 \log \frac{4ET}{\mu^2} \longrightarrow \alpha_s(\mu^2) \alpha_s(4ET) \log \frac{4ET}{\mu^2(\alpha_s(4T^2); T)}$$

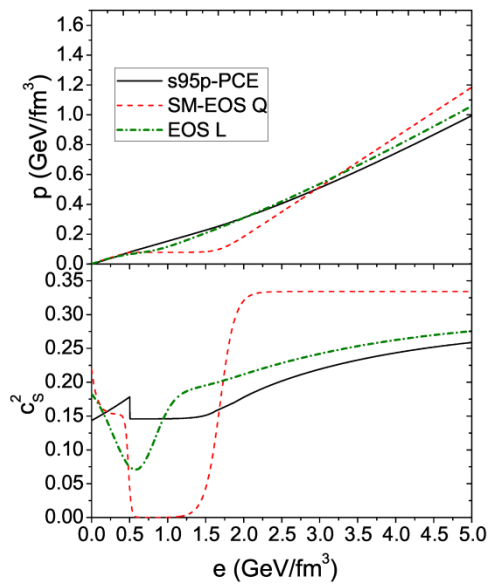
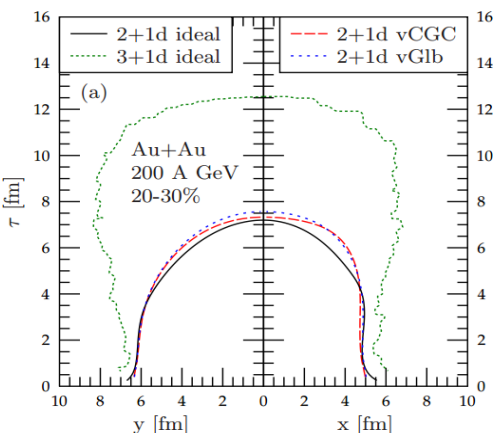
# Radiative Running Coupling Effects at LHC via CUJET1.0



❖ Running coupling CUJET fits (by eye ball) the pion RAA of RHIC and LHC with the same maximum coupling 0.4 in a Glauber transverse + Bjorken longitudinal profile, but RAA's low  $p_T$  rising and high  $p_T$  saturating behavior is not manifest enough



# CUJET2.0 = rcDGLV + Elastic + 2+1D Viscous Hydro

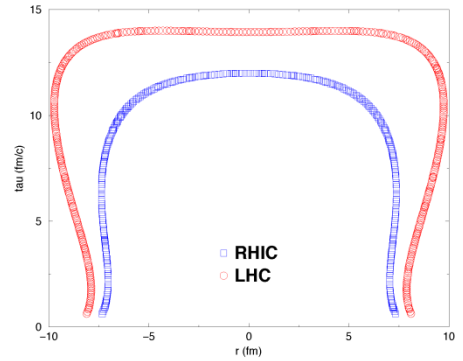
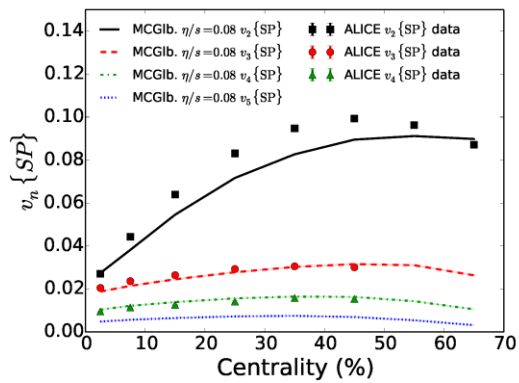


- ❖ Couple rcDGLV to VISH 2+1D expanding QGP fluid fields ( $T(x,t), v(x,t)$ )

- ❖ RHIC Au+Au 200AGeV & LHC Pb+Pb 2.76ATeV

- Equation of State: s95p-v0-PCE
- Initial Condition: MC-Glauber
- $\eta/s=0.08$
- Initial Time: 0.6fm/c
- Cooper-Frye freeze-out temperature: 120MeV

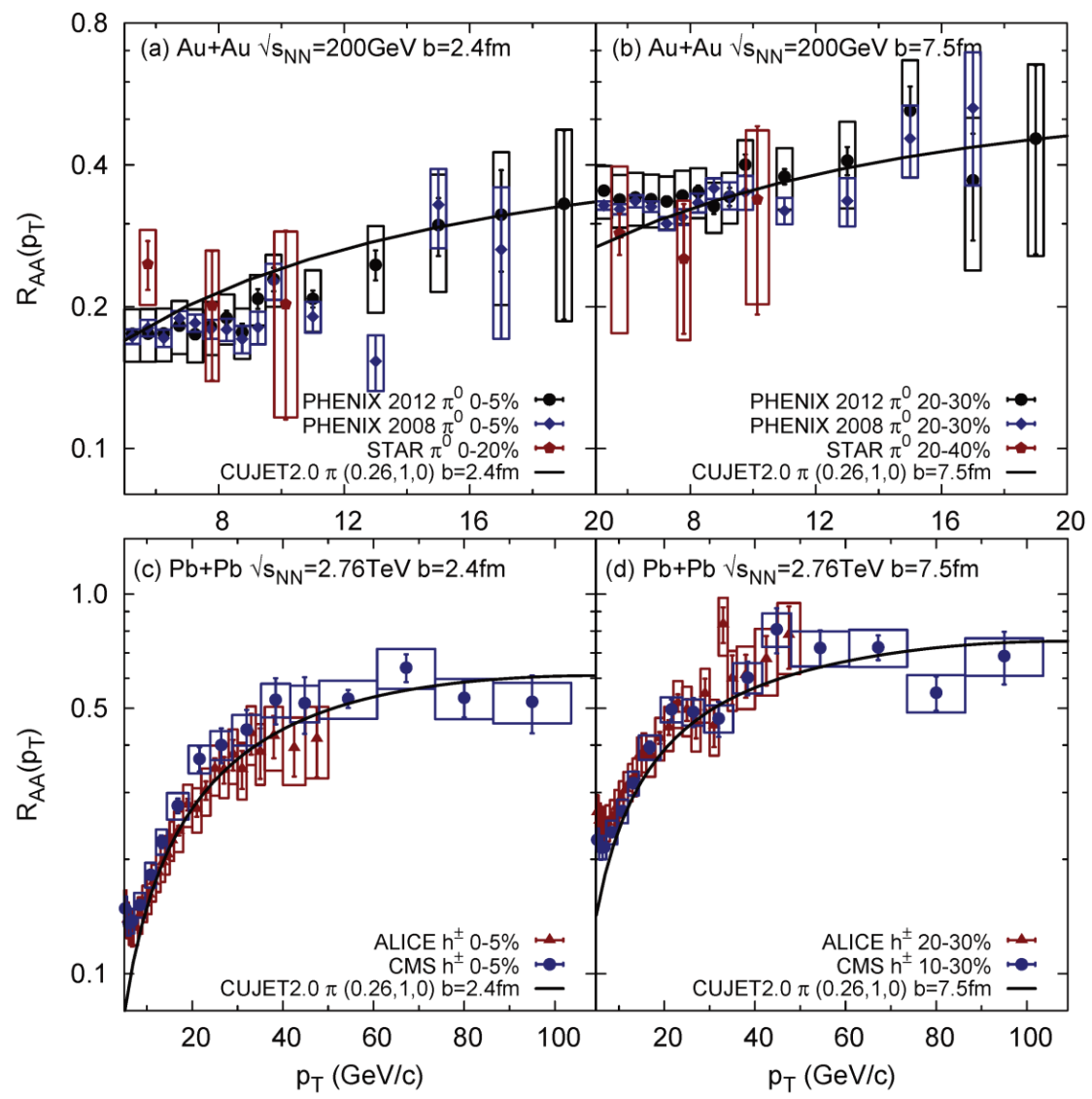
- ❖ Compatible with measurements of low pT particle production spectra and flow harmonics



T. Renk, H. Holopainen, U. Heinz and C. Shen, PRC 83, 014910 (2011)  
 C. Shen, U. Heinz, P. Huovinen and H. Song, PRC 82, 054904 (2010)  
 H. Song and U. Heinz, PRC 78, 024902 (2008)

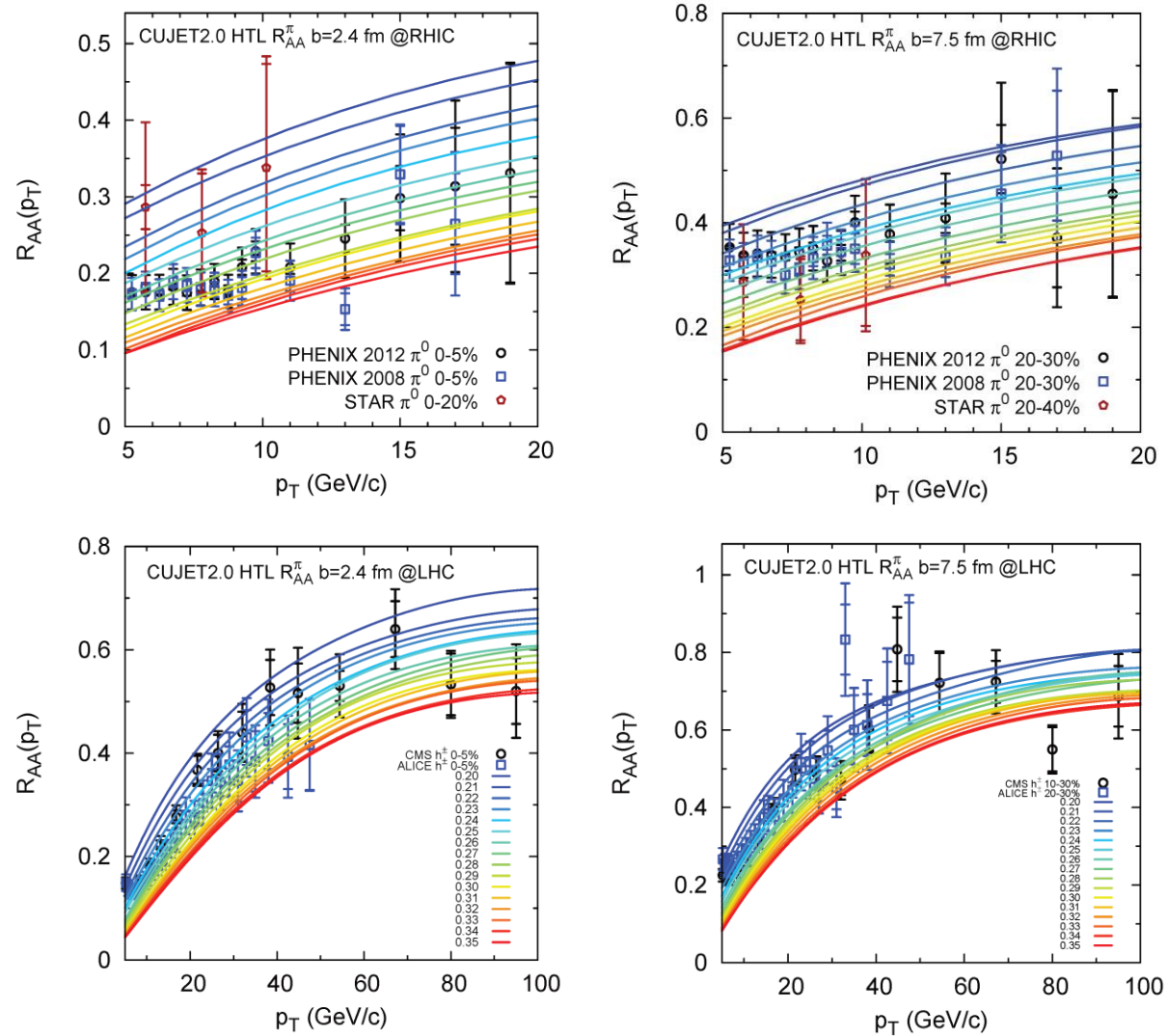
Chun Shen, Private Communication

# CUJET2.0 Result: $R_{AA}$ at RHIC and LHC



- ❖  $(\alpha_{max}, f_E, f_M) = (0.26, 1, 0)$
- ❖ The pion  $R_{AA}$  is compatible with both RHIC and LHC data in both central and semi-peripheral collisions
  - The same choice of running coupling but with a different medium evolution background can still explain the surprising transparency at LHC
- ❖ Clearer tendency of  $R_{AA}$  flattening at high  $p_T$
- ❖ The coupling strength significantly decreases in a transverse expanding medium comparing to the static case
  - Comparing to a static medium, longer jet path length in a transverse expanding medium compensates the reduction in density and results in overall enhanced quenching

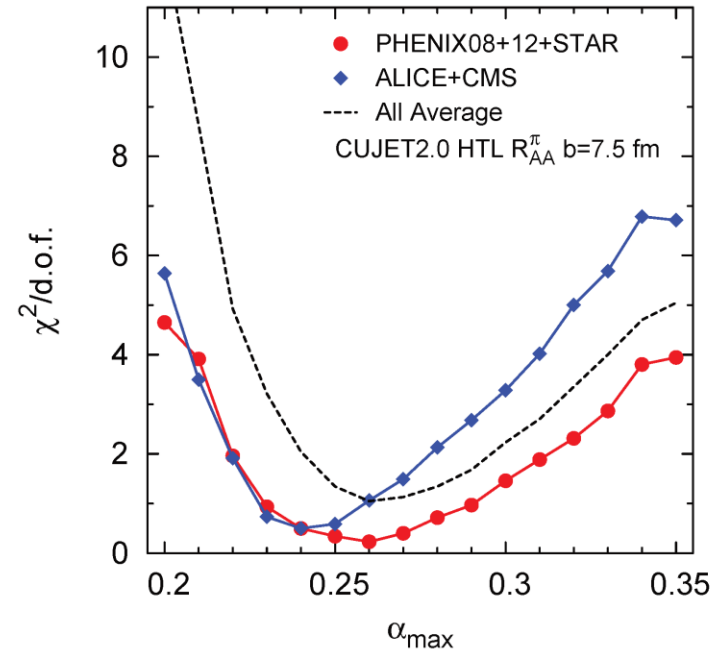
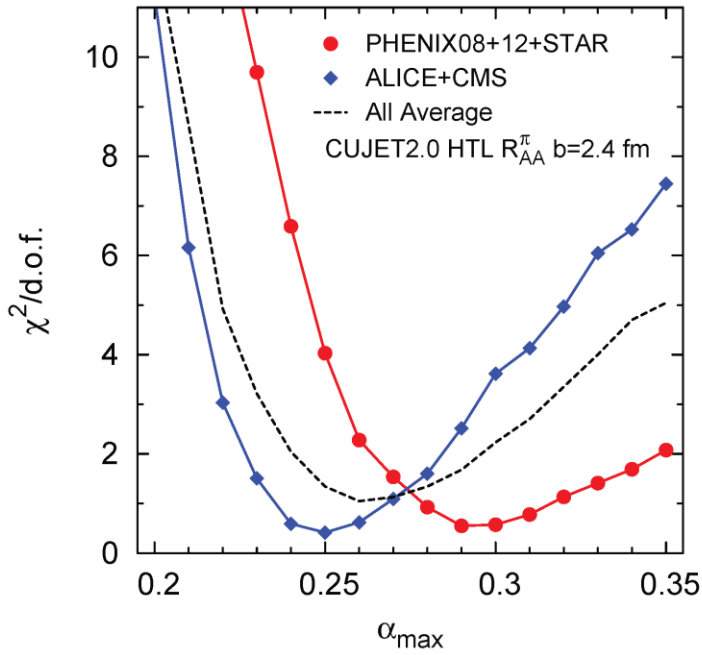
*Fits by eyeball are not good enough, need chi^2 to quantify*



The JET Collaboration, arXiv:1312:5003

- ❖ Chi^2 analysis is necessary to determine the best fit  $a_{max}$  value, we choose to compare data above 8GeV/c
- ❖ At low  $a_{max}$  the increment in RAA is near uniform  $\rightarrow$  asymptotically the fixed coupling limit
- ❖ Band width remains almost the same at RAA flattening region  $\rightarrow$  for high  $p_T$   $r_c$  is less important than expanding medium

*Fits by eyeball are not good enough, need  $\chi^2$  to quantify*



The JET Collaboration, arXiv:1312:5003

$\alpha_{max}$	RHIC $\tilde{\chi}^2 < 1$	LHC $\tilde{\chi}^2 < 1$	RHIC $\tilde{\chi}^2 < 2$	LHC $\tilde{\chi}^2 < 2$
$b = 2.4$ fm	0.28-0.32	0.24-0.27	0.26-0.35	0.23-0.28
$b = 7.5$ fm	0.23-0.29	0.23-0.25	0.22-0.31	0.22-0.27

- $\alpha_{max} = 0.26 - 0.27$ , if limit  $\chi^2/d.o.f. < 2$  separately
- $\alpha_{max} = 0.25 - 0.27$ , if average  $\chi^2/d.o.f. < 1.5$

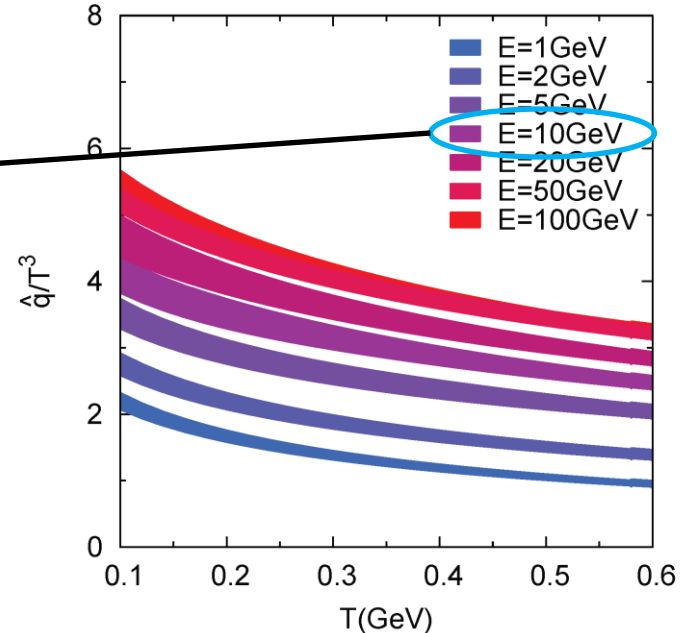
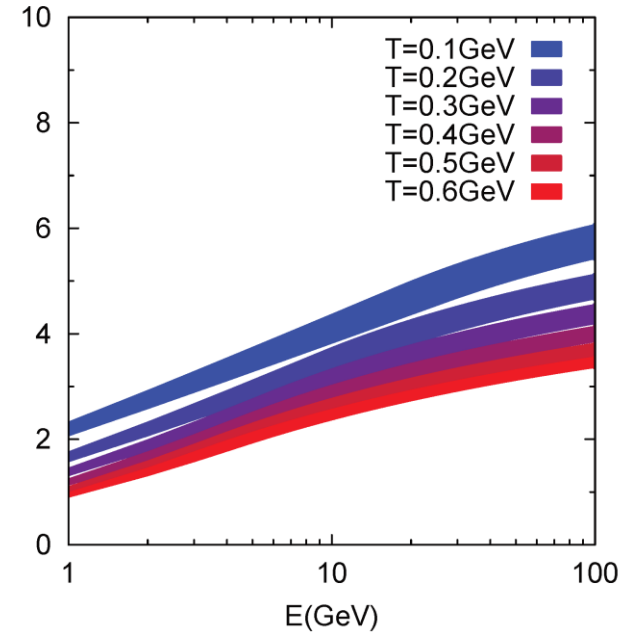
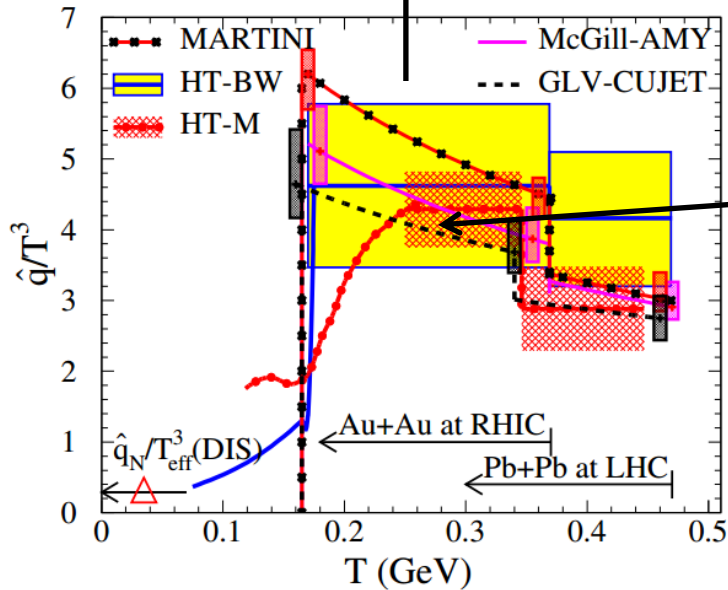
# Jet Transport Coefficient in CUJET2.0

$$\hat{q}(E, T; \alpha_{max}, f_E, f_M) = \rho(T) \int_0^{4ET} d\mathbf{q}^2 \mathbf{q}^2 \frac{d\sigma_{\text{eff}}}{d\mathbf{q}^2}$$

$$\frac{d\sigma_{\text{eff}}}{d\mathbf{q}^2} = \frac{\alpha_s^2(\mathbf{q}^2)(f_E^2 - f_M^2)}{(\mathbf{q}^2 + f_E^2 \mu^2(T))(\mathbf{q}^2 + f_M^2 \mu^2(T))}$$

$$\mu(T) = T \sqrt{4\pi\alpha_s(4T^2)(1 + n_f/6)}$$

$$\frac{\hat{q}}{T^3} \approx \begin{cases} 4.6 \pm 1.2 & \text{at RHIC,} \\ 3.7 \pm 1.4 & \text{at LHC,} \end{cases}$$

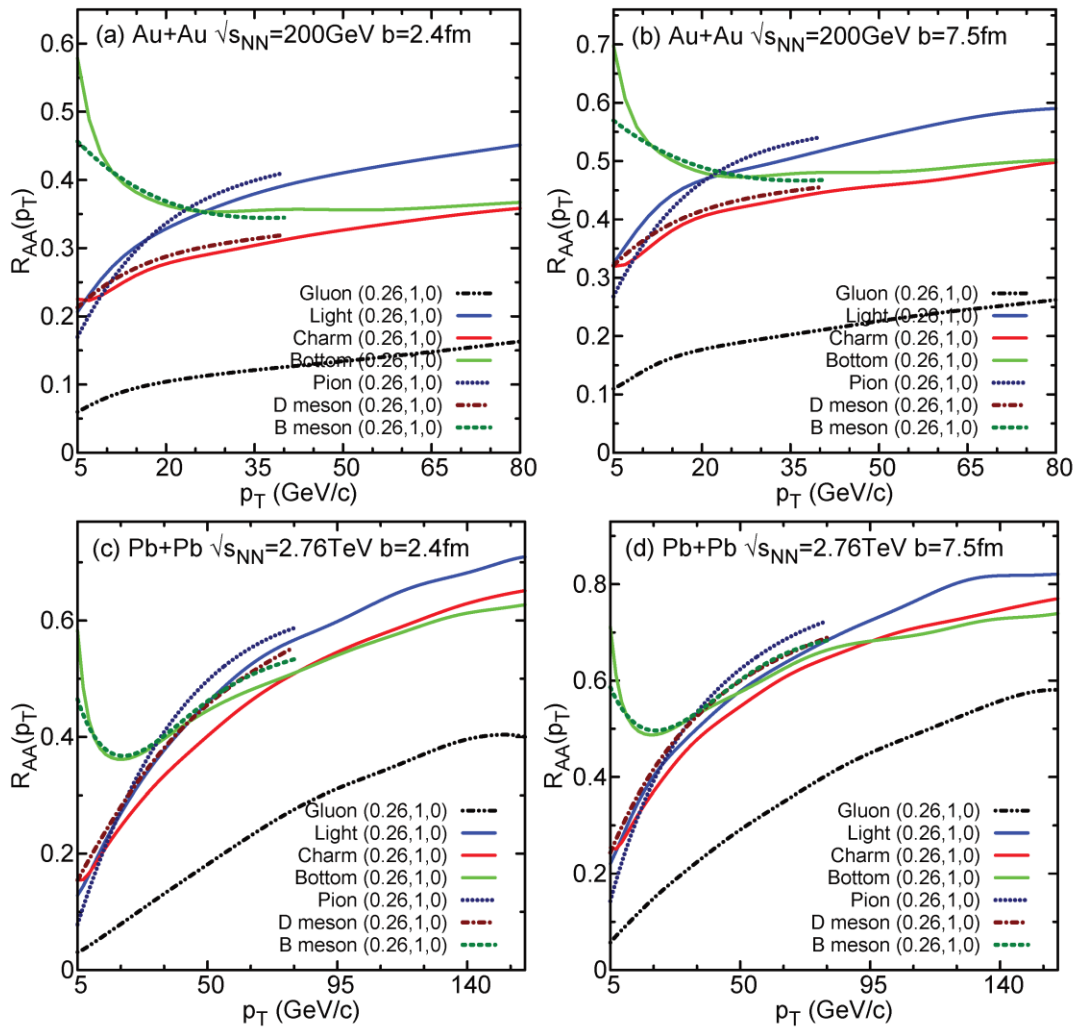


The JET Collaboration, arXiv:1312:5003

# Outline

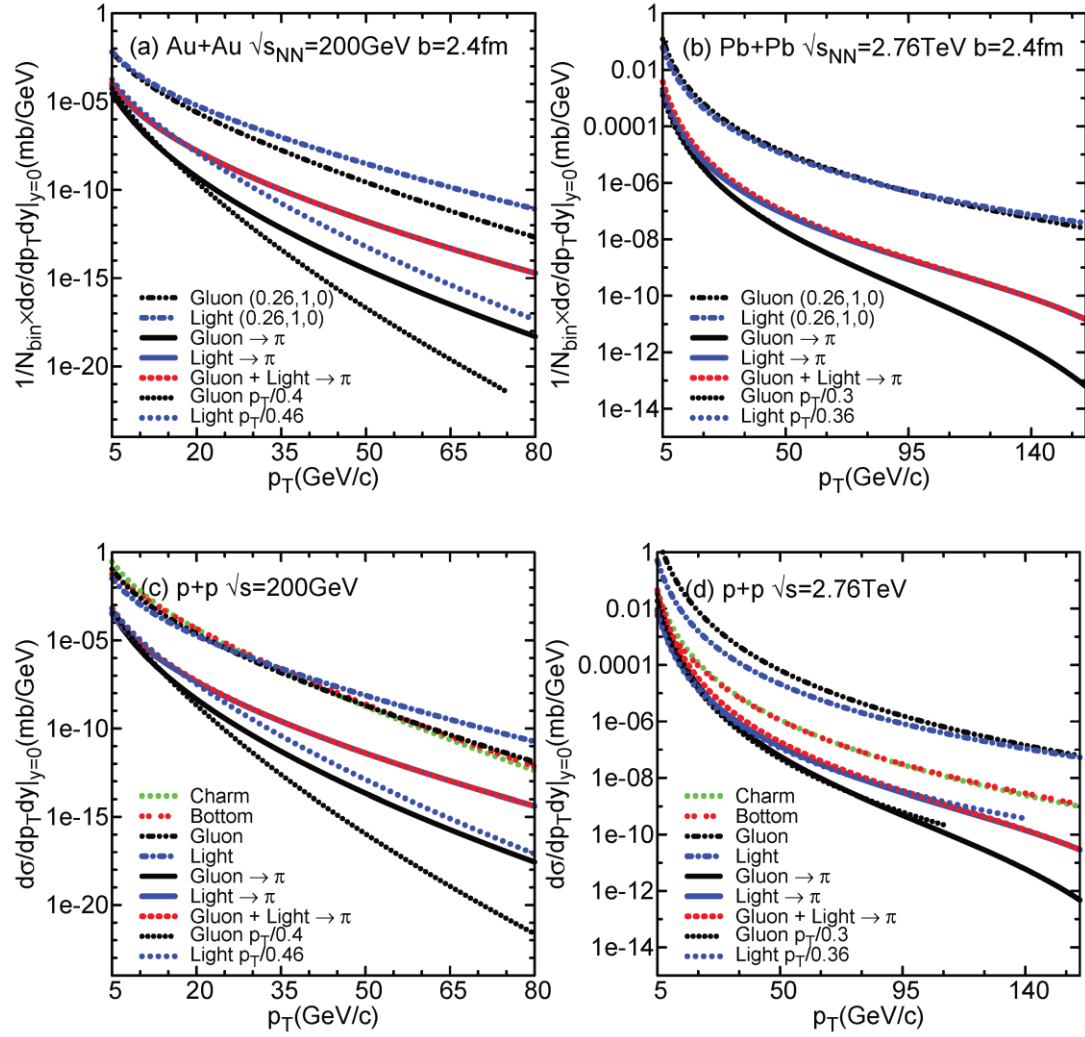
- ❖ Part I: CUJET2.0: A pQCD Model for Azimuthal Jet Flavor Tomography at RHIC and LHC
  - Radiative jet energy loss in QGP: (D)GLV Opacity Expansion
  - Pre-CUJET: WHDG/DGLV, heavy quark puzzle
  - CUJET1.0 = dynamical fixed coupling DGLV + elastic + trans. Glauber & long. Bjorken
  - The surprising transparency of QGP at LHC, multi-scale running strong coupling
  - CUJET2.0 = dynamical running coupling DGLV + elastic + 2+1D viscous hydro
  - CUJET2.0 results on pion/charged hadron RAA and jet transport coefficient
- ❖ Part II: CUJET2.0 Jet Quenching Phenomenology
  - Why light quark and charged hadron RAA at RHIC and LHC are almost the same?
  - Heavy flavor RAA
  - Why pion and beauty RAA have an crossover?
- ❖ Part III: The jet  $v_2$  open problem
  - Puzzle: consistency with (RAA &  $v_2$ ) AND (RHIC & LHC) AND (central & peripheral)
  - CUJET2.0: reaction plane dependent jet quenching pattern
  - CUJET2.0: light flavor  $v_2$
  - CUJET2.0: heavy flavor  $v_2$
- ❖ Summary and Outlook

# Partonic and Hadronic RAA vs $p_T$ at RHIC and LHC



❖ Light quark RAA and pion/charged hadron RAA are almost the same at both RHIC and LHC, despite the fact that at LHC the gluon production is larger than quark

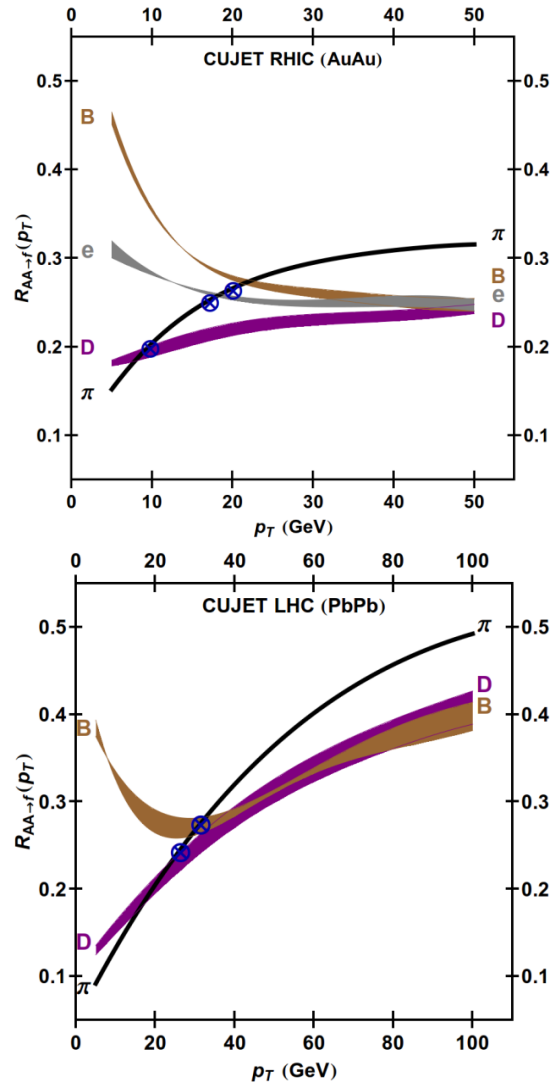
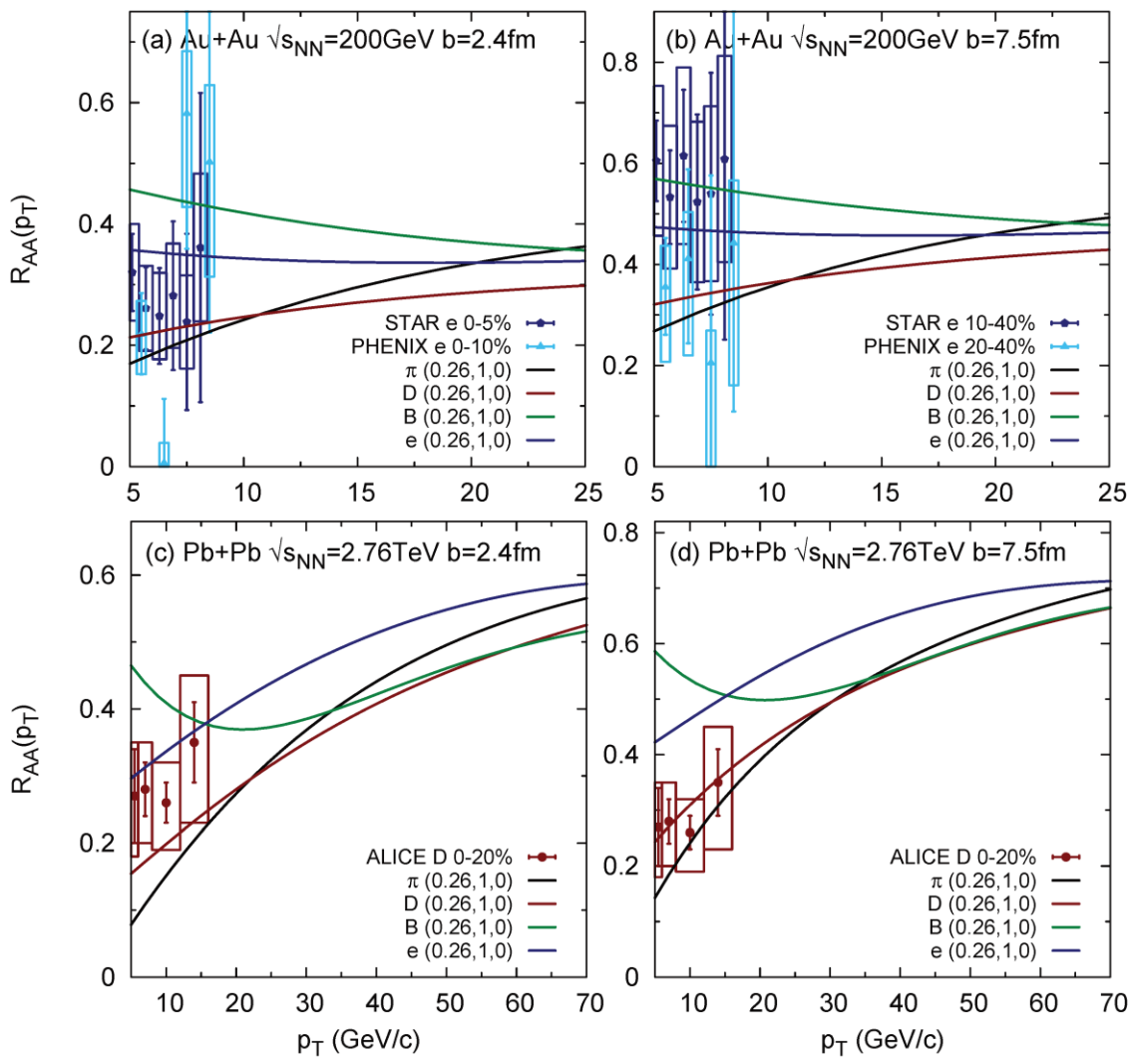
# Similarity between light quark and pion RAA at RHIC and LHC



- ❖ Larger Casimir for gluon ( $C_R=3$ ) than quark ( $C_R=4/3$ ) leads to more energy loss for the gluon, brings their AA production spectra at LHC to the same level
- ❖ Different fragmentation ratios of gluon and quark to pion make the light quark's contribution to pion AA spectrum dominant



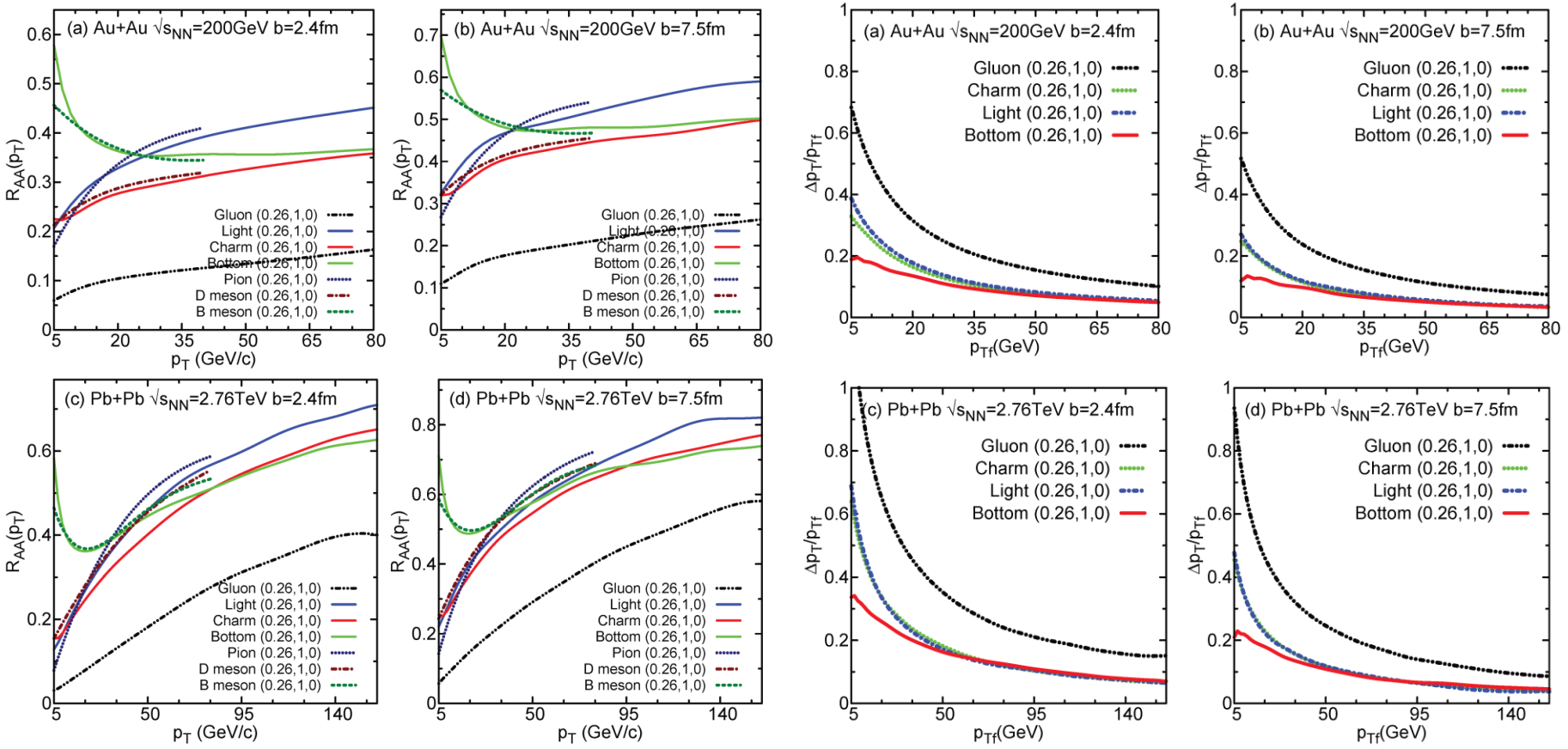
# CUJET2.0 Result: Heavy Flavor at RHIC and LHC



Buzzatti and Gyulassy, PRL (2012)

- ❖ Both CUJET1.0 and 2.0 solve “Heavy Quark Puzzle”, suggesting the importance of realistic path length fluctuation, no approximation of initial production spectra and include dynamical QCD medium effect
- ❖ RAA crossing pattern insensitive to running coupling and medium evolution profile  $\rightarrow$  Mass ordering encoded in DGLV+TG
- ❖ At low  $p_T$ , charm and pion mixed together, beauty RAA is well above them

# Why pion and beauty RAA have a level crossing?



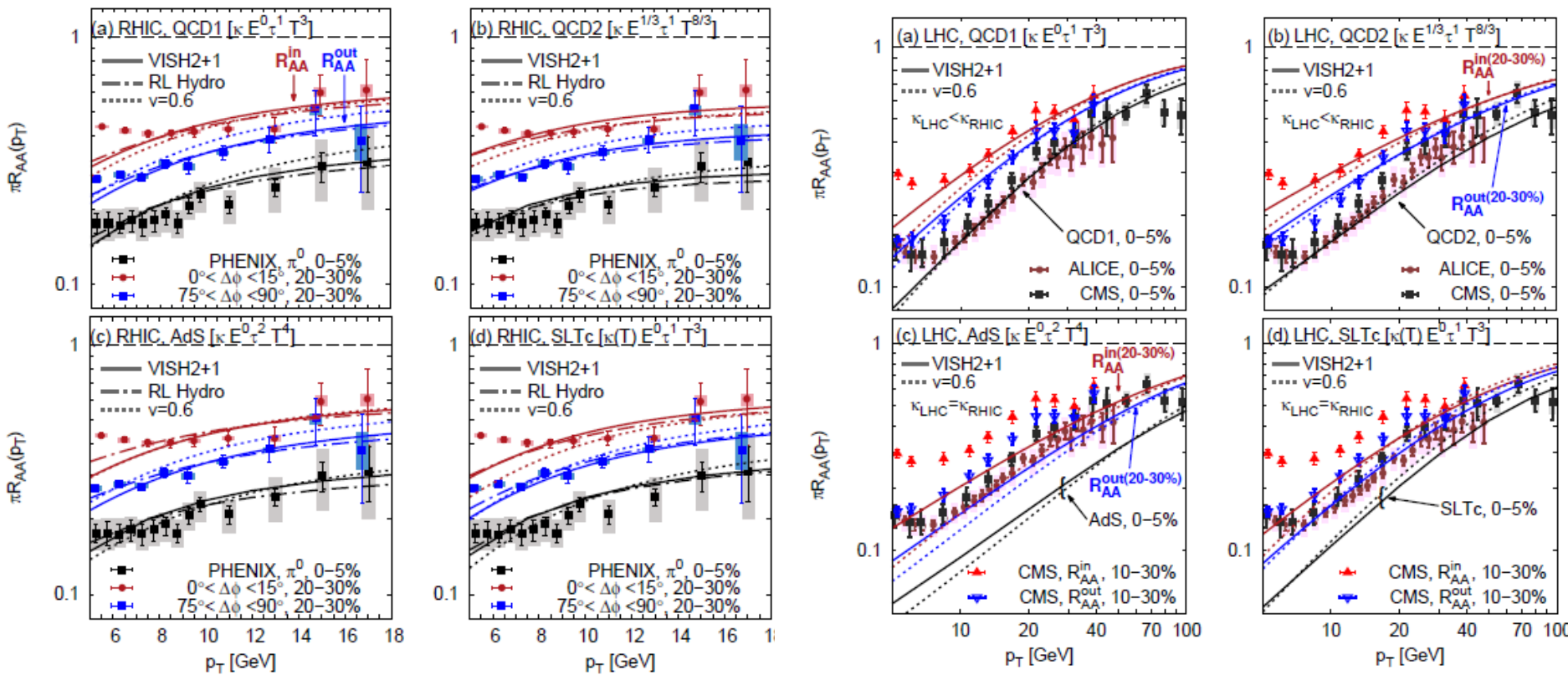
$$\frac{d\sigma^{AA \rightarrow h}}{d^3 p_f} \equiv \frac{1}{N_{bin}} \frac{d\sigma^{AA \rightarrow h}}{d^3 p_f} = \frac{d\sigma^{pp \rightarrow q}}{d^3 p_i} \otimes P(E_i(p_i) \rightarrow E_f(p_f)) \otimes D(q \rightarrow h)$$

❖ The pp spectrum and partonic energy loss theory combined to lead to the level crossing, and the former plays a more critical role

# Outline

- ❖ Part I: CUJET2.0: A pQCD Model for Azimuthal Jet Flavor Tomography at RHIC and LHC
  - Radiative jet energy loss in QGP: (D)GLV Opacity Expansion
  - Pre-CUJET: WHDG/DGLV, heavy quark puzzle
  - CUJET1.0 = dynamical fixed coupling DGLV + elastic + trans. Glauber & long. Bjorken
  - The surprising transparency of QGP at LHC, multi-scale running strong coupling
  - CUJET2.0 = dynamical running coupling DGLV + elastic + 2+1D viscous hydro
  - CUJET2.0 results on pion/charged hadron RAA and jet transport coefficient
- ❖ Part II: CUJET2.0 Jet Quenching Phenomenology
  - Why light quark and charged hadron RAA at RHIC and LHC are almost the same?
  - Heavy flavor RAA
  - Why pion and beauty RAA have an crossover?
- ❖ Part III: The jet  $v_2$  open problem
  - Puzzle: consistency with (RAA &  $v_2$ ) AND (RHIC & LHC) AND (central & peripheral)
  - CUJET2.0: reaction plane dependent jet quenching pattern
  - CUJET2.0: light flavor  $v_2$
  - CUJET2.0: heavy flavor  $v_2$
- ❖ Summary and Outlook

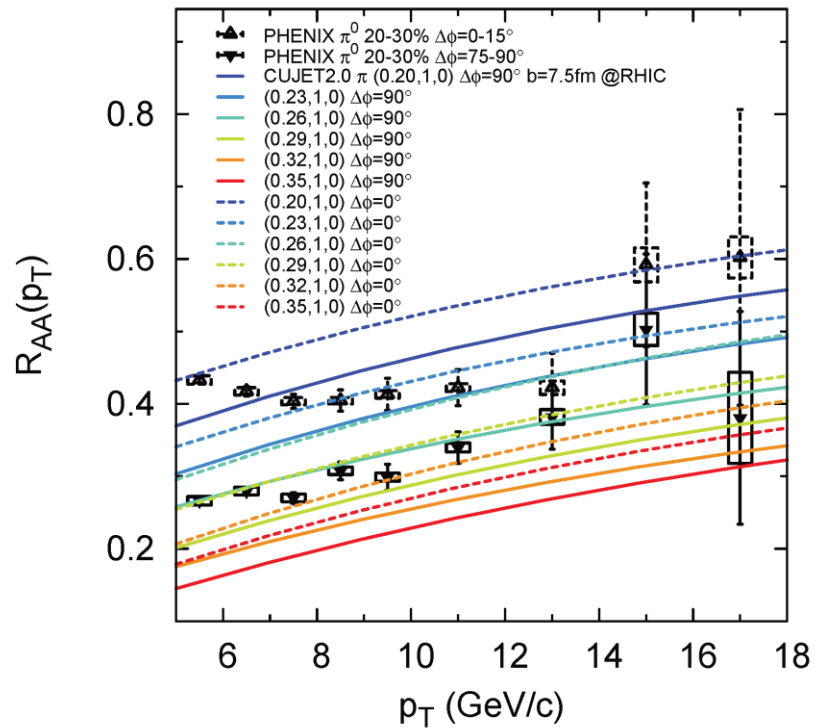
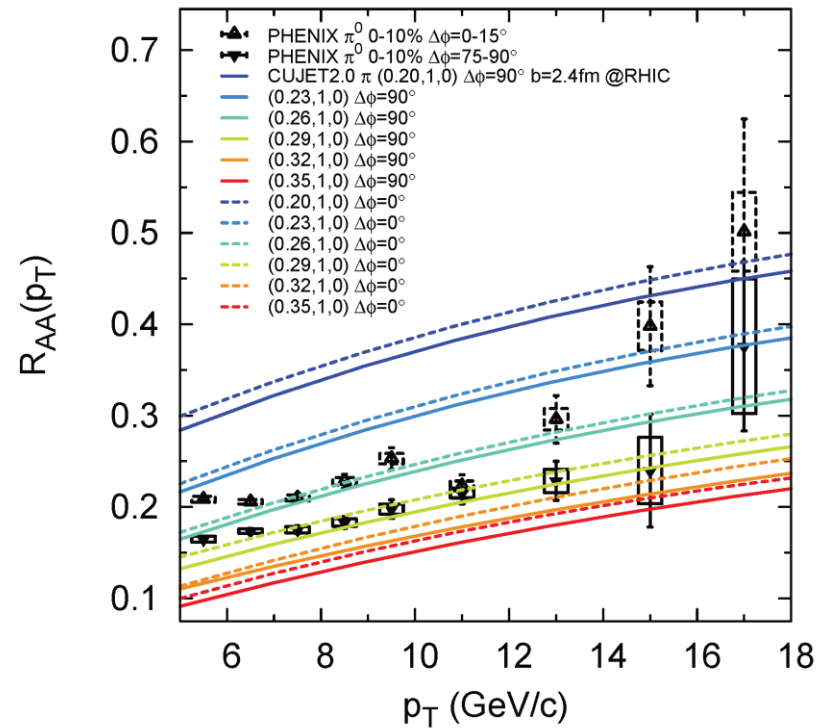
# Consistency with (RAA & $v_2$ ) AND (RHIC & LHC) AND (central & peripheral)



- ❖ B. Betz and M. Gyulassy, arXiv:1305.6458
  - QCD1 → rcCUJET1.0; QCD2 → fcCUJET1.0; AdS → fixed t'Hooft conformal falling string; SLTc → Shuryak-Liao assuming  $T_c$  dominated
  - VISH2+1-Shen,Heinz,Song; RL-Romatschke,Luzum
  - QCD1 (0,1,3) (WITHOUT energy loss fluctuation) is the simplest minimal dEdx phenomenology compatible with all 8 combinations of jet quenching data
- ❖ D. Molnar and S. Deke, arXiv:1305.1046
  - $R_{AA}$  and  $v_2$  cannot be satisfied with the same set of parameters in MPC+GLV

# CUJET2.0 Result: pion suppression factor w.r.t. reaction plane

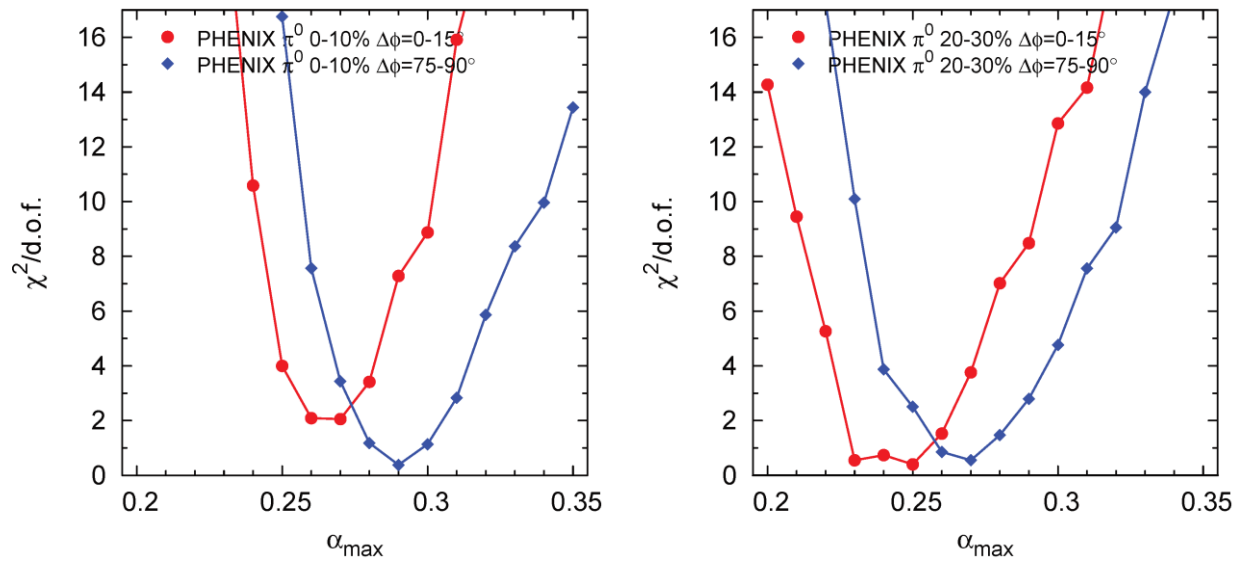
$$\frac{dN_h}{dydp_T d\phi} = \frac{dN_h}{dydp_T} \frac{1}{2\pi} (1 + 2v_1 \cos \phi + 2v_2 \cos 2\phi + \dots) \longrightarrow \begin{cases} R_{AA}^{in}(y, p_T) = \frac{\frac{dN_h^{AA}}{dydp_T d\phi} |_{\phi=0}}{N_{binary} \frac{dN_h^{pp}}{dydp_T d\phi} |_{\phi=0}} = \frac{\frac{dN_h^{AA}}{dydp_T} \frac{1}{2\pi} (1 + 2v_1 + 2v_2 + \dots)}{N_{binary} \frac{dN_h^{pp}}{dydp_T d\phi} |_{\phi=0}} \\ R_{AA}^{out}(y, p_T) = \frac{\frac{dN_h^{AA}}{dydp_T d\phi} |_{\phi=\frac{\pi}{2}}}{N_{binary} \frac{dN_h^{pp}}{dydp_T d\phi} |_{\phi=\frac{\pi}{2}}} = \frac{\frac{dN_h^{AA}}{dydp_T} \frac{1}{2\pi} (1 - 2v_2 - \dots)}{N_{binary} \frac{dN_h^{pp}}{dydp_T d\phi} |_{\phi=\frac{\pi}{2}}} \end{cases}$$



$\alpha_{max}$	RHIC $\tilde{\chi}^2 < 1$	LHC $\tilde{\chi}^2 < 1$	RHIC $\tilde{\chi}^2 < 2$	LHC $\tilde{\chi}^2 < 2$
$b = 2.4$ fm	0.28-0.32	0.24-0.27	0.26-0.35	0.23-0.28
$b = 7.5$ fm	0.23-0.29	0.23-0.25	0.22-0.31	0.22-0.27

- ❖ No  $\alpha_{max}$  can reproduce the gap between  $R_{AA}^{in}$  and  $R_{AA}^{out}$  at RHIC
- ❖ Recall the  $\tilde{\chi}^2 < 2$  spans a  $p_T$  range for each collision  $\rightarrow$  What is the best  $v_2$  within uncertainty?

# CUJET2.0 Result: pion suppression factor w.r.t. reaction plane



$\alpha_{max}$	RHIC $\tilde{\chi}^2 < 1$	LHC $\tilde{\chi}^2 < 1$	RHIC $\tilde{\chi}^2 < 2$	LHC $\tilde{\chi}^2 < 2$
$b = 2.4$ fm	0.28-0.32	0.24-0.27	0.26-0.35	0.23-0.28
$b = 7.5$ fm	0.23-0.29	0.23-0.25	0.22-0.31	0.22-0.27

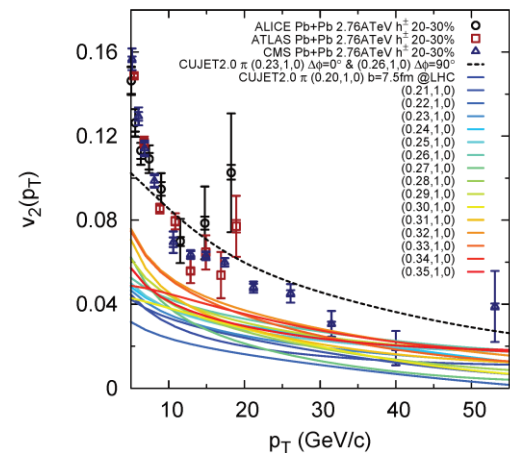
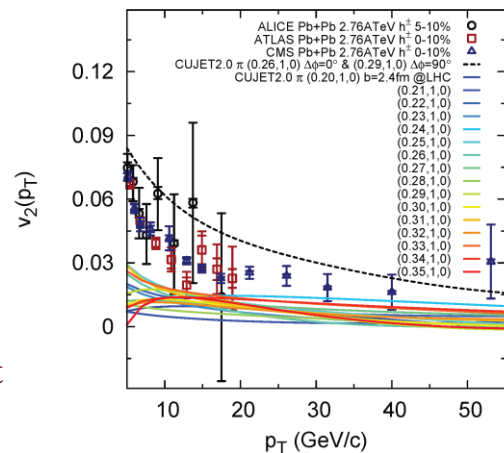
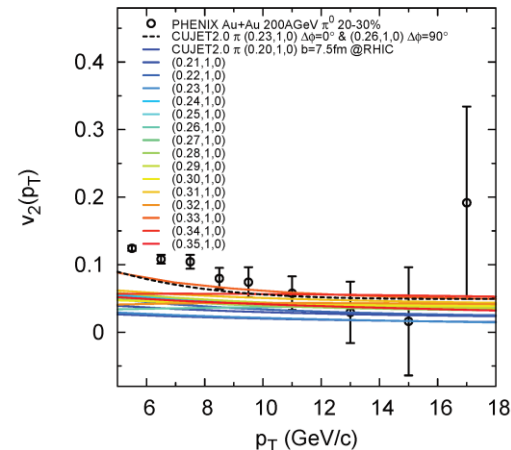
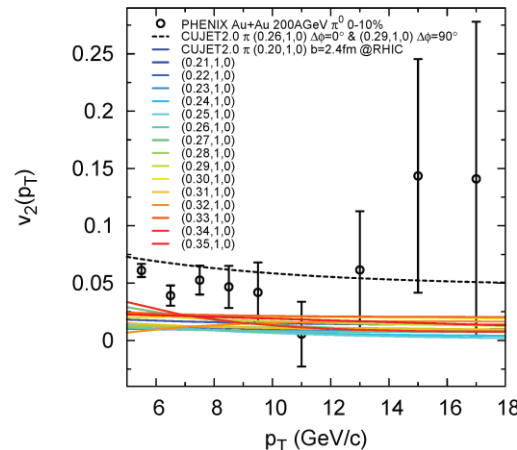
- Choose  $\alpha_{max} = 0.23$  ( $7.5\text{fm} + IN$ ),  $0.26$  ( $7.5\text{fm} + OUT$ ),  $0.26$  ( $7.5\text{fm} + IN$ ),  $0.29$  ( $7.5\text{fm} + OUT$ ), the average  $R_{AA}$  falls within respective  $\chi^2/d.o.f. < 2$  window, while  $R_{AA}^{in}$  and  $R_{AA}^{out}$  are in perfect agreements with RHIC data
- As less as 10% azimuthal variation of path averaged  $\alpha_{max}$  can account for the underestimated gap between  $R_{AA}^{in}$  and  $R_{AA}^{out}$  at RHIC
- Interesting ordering: in terms of naive path length from the origin,  $7.5\text{fm} + IN < 7.5\text{fm} + OUT \approx 2.4\text{fm} + IN < 2.4\text{fm} + OUT$ , the corresponding  $\alpha_{max}$ :  $0.23 < 0.26 = 0.26 < 0.29$ .
- Model is fully constrained at RHIC, how about extrapolation to LHC?

# CUJET2.0 Result: pion $v_2$

$$\begin{cases} R_{AA}^{in}(p_T) \approx \frac{dN_h^{AA}}{dydp_T} (1 + 2v_2 + 2v_4 \dots) \\ R_{AA}^{out}(p_T) \approx \frac{dN_h^{AA}}{dydp_T} (1 - 2v_2 - 2v_4 \dots) \end{cases} = R_{AA}^h (1 + 2v_2 + 2v_4 \dots) ,$$

$$\begin{cases} R_{AA}^{in}(p_T) \approx R_{AA}^h (1 + 2v_2) , \\ R_{AA}^{out}(p_T) \approx R_{AA}^h (1 - 2v_2) , \end{cases}$$

$$v_2(p_T) = \frac{1}{2} \frac{R_{AA}^{in}(p_T) - R_{AA}^{out}(p_T)}{R_{AA}^{in}(p_T) + R_{AA}^{out}(p_T)}$$



## ❖ Extrapolation to LHC fits $v_2$ !

- RAA is compatible with data in this anisotropic amax scenario as well
- As less as **10%** azimuthal variation in jet path averaged strong coupling can render **simultaneous fit of RAA and  $v_2$**
- This magnitude of variation is very modest in comparison to Shuryak-Liao huge non-perturbative near  $T_c$  enhancement of the effective jet medium coupling

❖ On the other hand, given this sensitivity of  $v_2$  on amax, calculating the exact running scales in GLV are important

- NLO or BLM?

$\chi^2/d.o.f.$ ( $b = 7.5$ fm)	$v_2$ , RHIC	$v_2$ , LHC	$R_{AA}$ , RHIC	$R_{AA}$ , LHC
$\alpha_{max}^{in} = 0.23, \alpha_{max}^{out} = 0.23$	3.72	43.03	0.93	0.73
$\alpha_{max}^{in} = 0.26, \alpha_{max}^{out} = 0.26$	2.06	24.89	0.23	1.06
$\alpha_{max}^{in} = 0.23, \alpha_{max}^{out} = 0.26$	0.50	4.92	0.42	0.54

# On the azimuthal angle dependence of maximum coupling constant in CUJET2.0

❖ Lattice QCD free energy of static qqbar pair

➤ Bazavov and Petreczky,  
 J.Phys.Conf.Ser.458 (2013) 012012 &  
 J.Phys.Conf.Ser.432 (2013) 012003

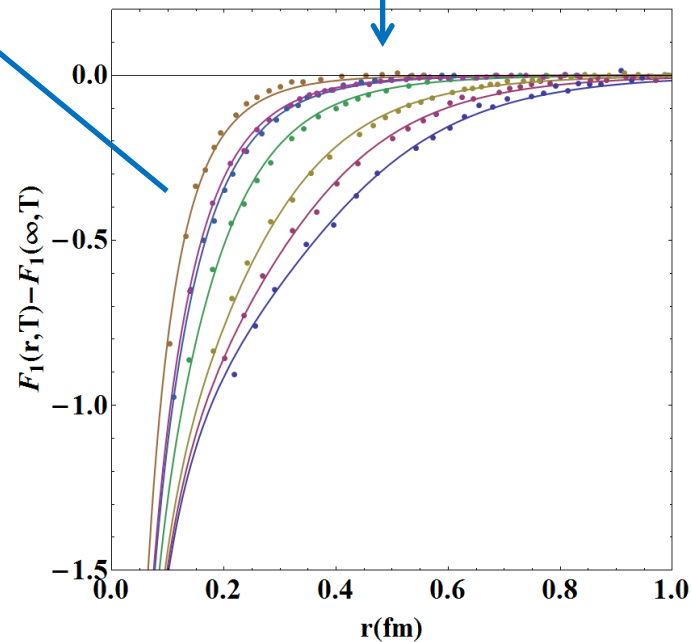
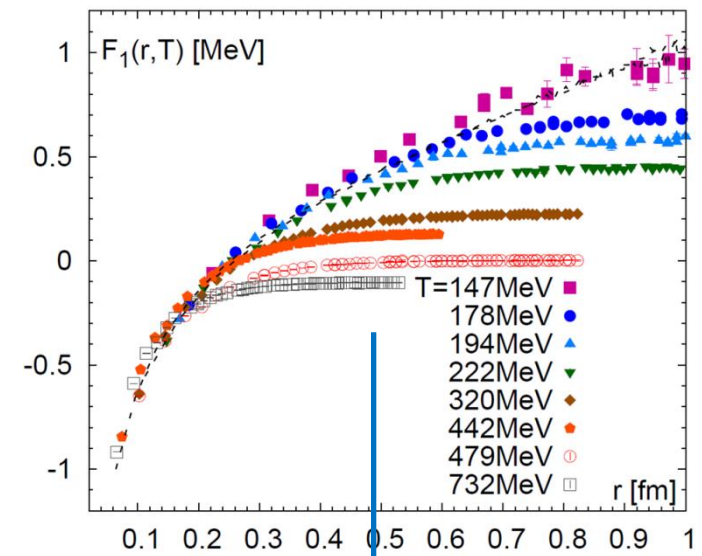
❖ Interpolate the form of effective potential and running coupling from lattice data

$$F_1(r, T) - F_1(\infty, T) = -\frac{0.71e^{-0.635T^{0.395}r}}{r \log\left[\left(\frac{0.35}{r}\right)^3 + \left(\frac{T}{156}\right)^3\right]}$$

$$\alpha_s(q, T(\mathbf{z} = \vec{x}_{0\perp} + \tau\hat{\phi})) \rightarrow \alpha_{max}(\hat{\phi})$$

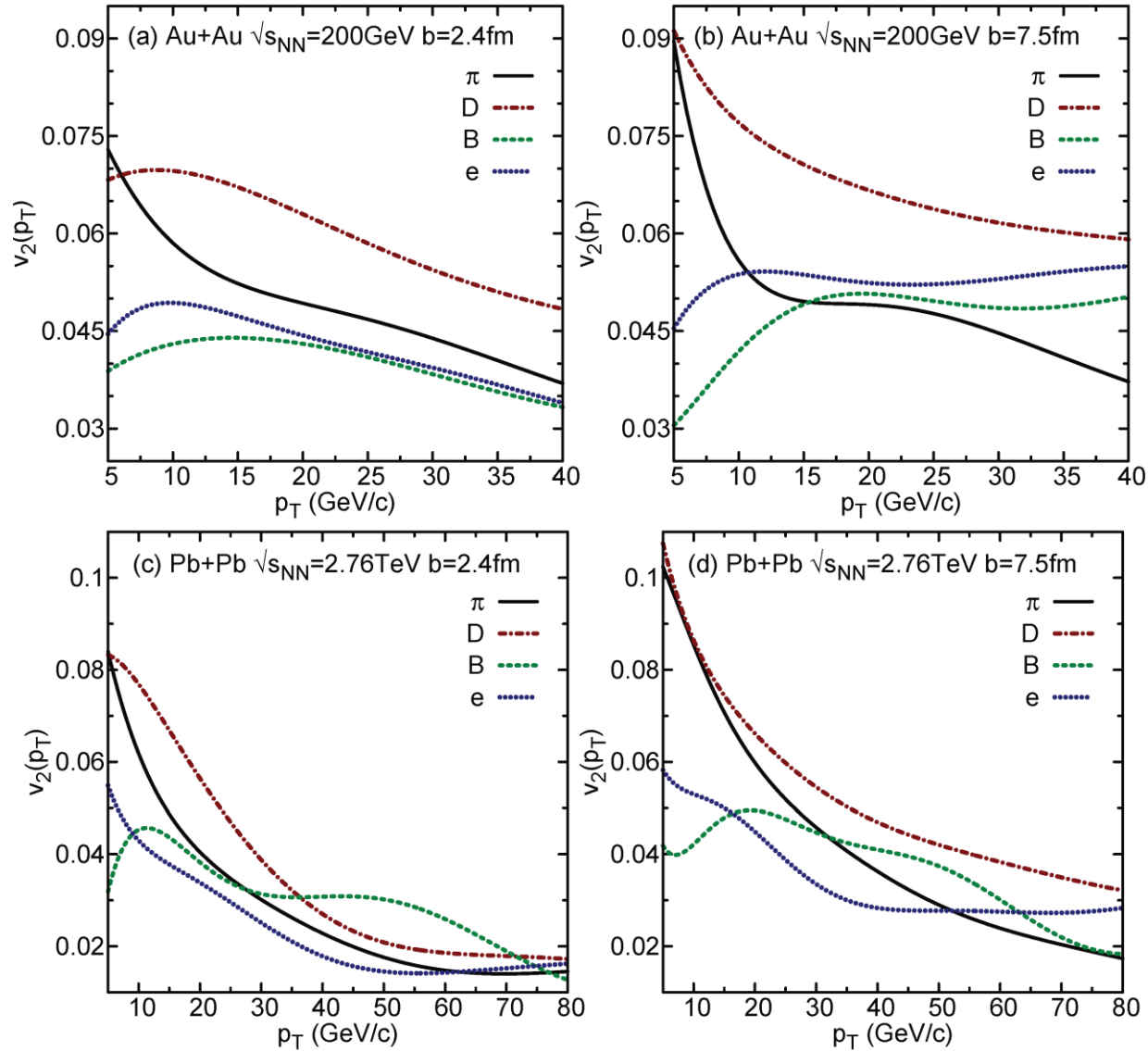
❖ The running strong coupling has local temperature dependence, since in present framework the coupling runs solely with energy, this local T effect may be reflected as azimuthal variation of path averaged maximum coupling

Bazavov and Petreczky, J.Phys.Conf.Ser.458 (2013) 012012 & 432 (2013) 012003





# CUJET2.0 Result: heavy flavor $v_2$



- ❖ B meson  $v_2$  has a peak at  $p_T \sim 10\text{GeV}$  @  $b=2.4\text{fm}$  and  $p_T \sim 20\text{GeV}$  @  $b=7.5\text{fm}$  at both RHIC and LHC
- ❖ Semi-ordering of the position of the peak for different flavor  $v_2$

# ***Outline***

- ❖ Part I: CUJET2.0: A pQCD Model for Azimuthal Jet Flavor Tomography at RHIC and LHC
  - Radiative jet energy loss in QGP: (D)GLV Opacity Expansion
  - Pre-CUJET: WHDG/DGLV, heavy quark puzzle
  - CUJET1.0 = dynamical fixed coupling DGLV + elastic + trans. Glauber & long. Bjorken
  - The surprising transparency of QGP at LHC, multi-scale running strong coupling
  - CUJET2.0 = dynamical running coupling DGLV + elastic + 2+1D viscous hydro
  - CUJET2.0 results on pion/charged hadron RAA and jet transport coefficient
- ❖ Part II: CUJET2.0 Jet Quenching Phenomenology
  - Why light quark and charged hadron RAA at RHIC and LHC are almost the same?
  - Heavy flavor RAA
  - Why pion and beauty RAA have an crossover?
- ❖ Part III: The jet  $v_2$  open problem
  - Puzzle: consistency with (RAA &  $v_2$ ) AND (RHIC & LHC) AND (central & peripheral)
  - CUJET2.0: reaction plane dependent jet quenching pattern
  - CUJET2.0: light flavor  $v_2$
  - CUJET2.0: heavy flavor  $v_2$
- ❖ **Summary and Outlook**

# Summary and Outlook

## Summary

- ❖ CUJET2.0 = running coupling DGLV + Elastic + 2+1D Viscous Hydro.
- ❖ CUJET can solve heavy quark energy loss puzzle mainly because of the inclusion of pQCD pp spectra and realistic path length fluctuations.
- ❖ After constrained all parameters at RHIC, CUJET2.0 can explain LHC charged hadron RAA's steep rising and subsequent flattening feature.
- ❖ CUJET2.0 predicts that beauty and pion/charged hadron RAA have a robust intersection which is largely resulted from the shape of the pp spectrum.
- ❖ As less as 10% azimuthal variation in path averaged strong coupling can gain simultaneous fit of both  $R_{AA}$  and  $v_2$  at both RHIC and LHC in both central and semi-peripheral collisions within the CUJET2.0 framework.

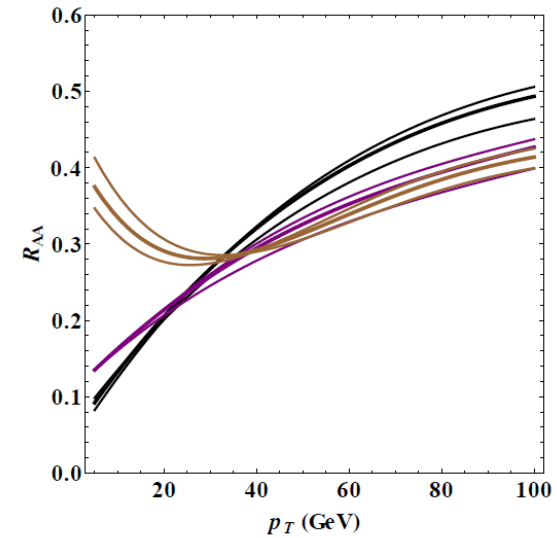
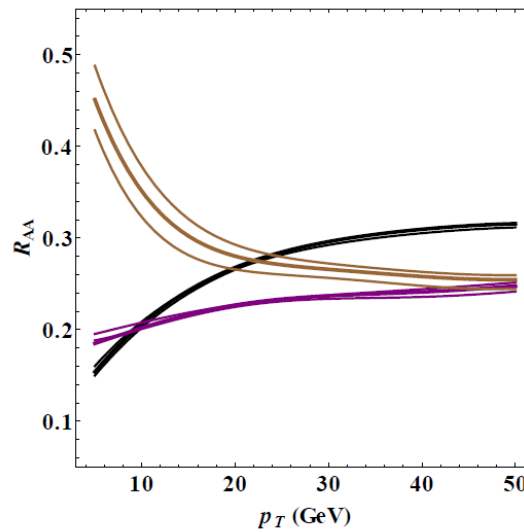
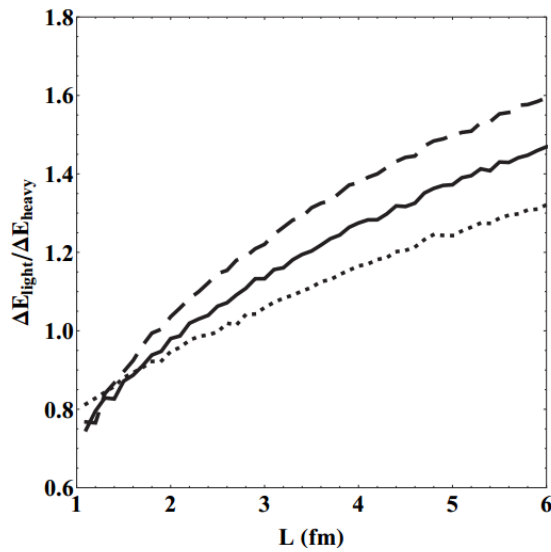
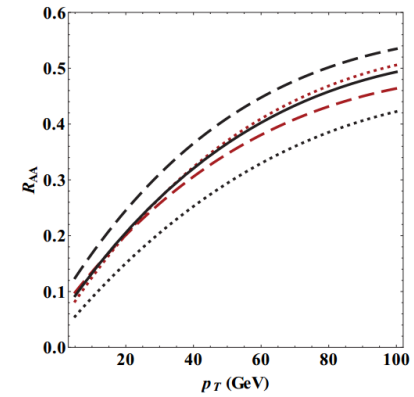
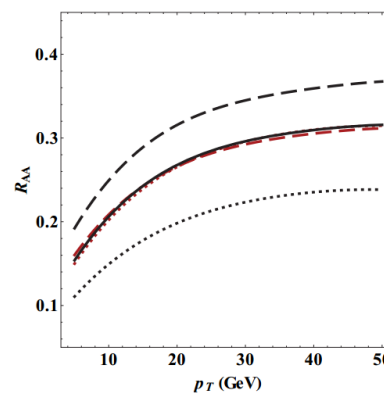
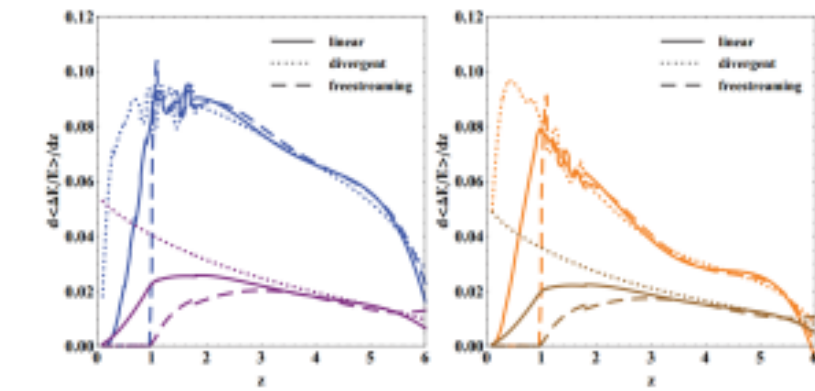
## Outlook

- ❖ Extrapolate an effective running coupling and scattering potential from lattice QCD data of non-perturbative qqbar potential  $V(r,T)$ , examine whether lattice QCD predicts the correct jet medium physics near  $T_c$ .
- ❖ Explore Shuryak-Liao magnetic monopole  $T_c$  enhancement picture in the CUJET2.0.
- ❖ Develop the algorithm to realize calculation of jet-hadron correlation observables in the CUJET.

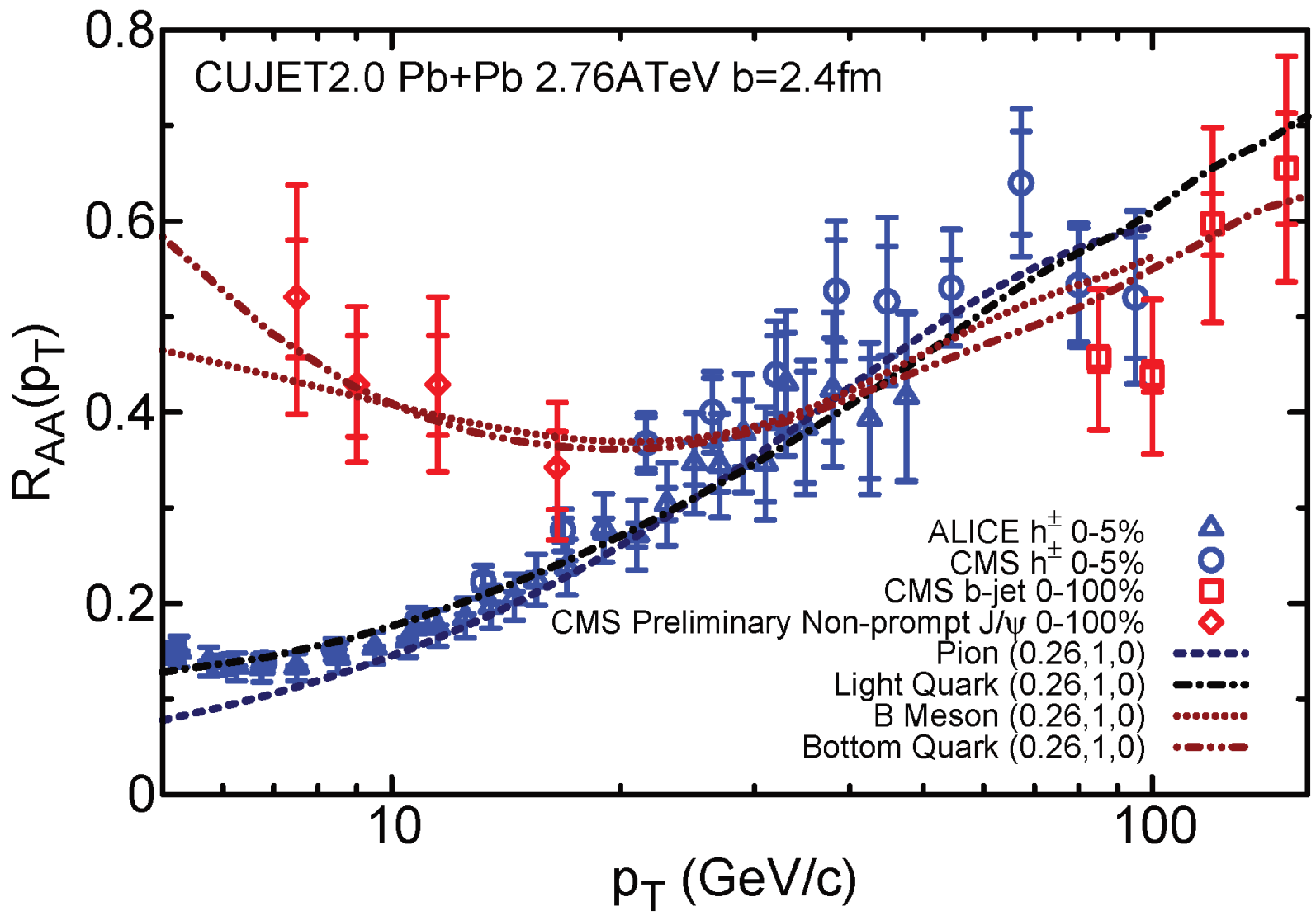
**Thank you!**

# *Backup*

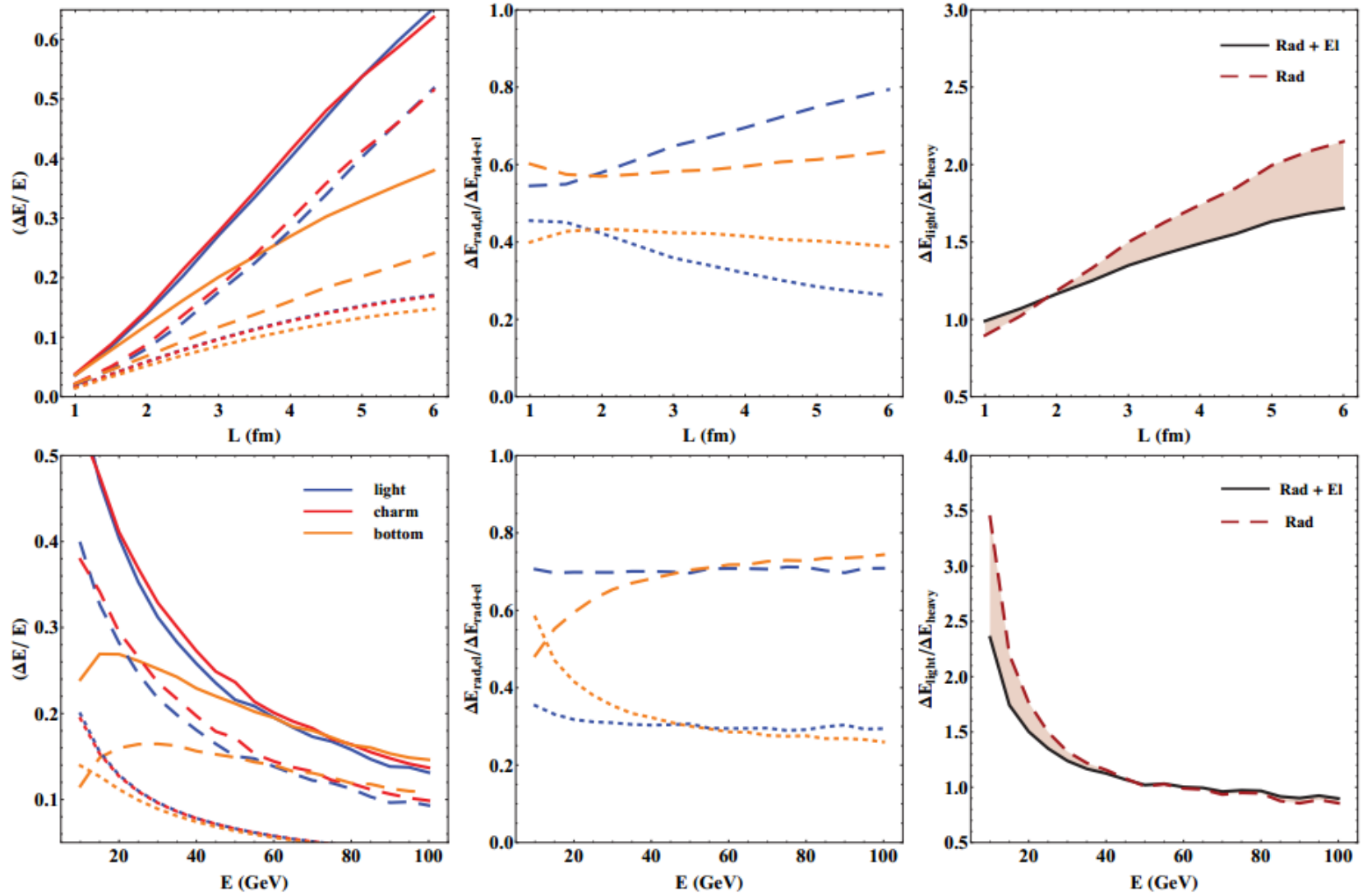
# Heavy Flavor – Pre-thermal Scheme



*Crossing*



# Radiative vs Elastic





# Higher Order in Opacity

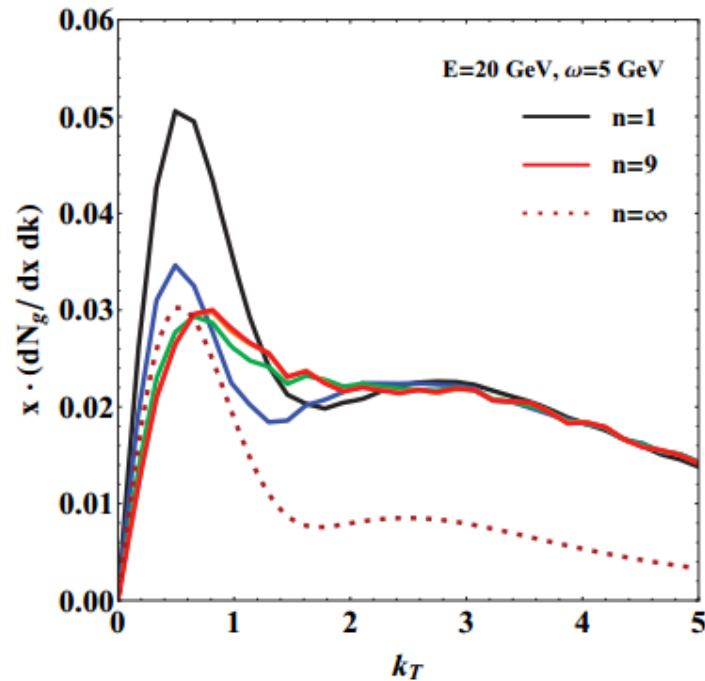


**Figure 15.** Radiated gluon transverse momentum distribution for a heavy quark jet with energy  $E = 20$  GeV traversing a brick plasma of size  $L = 5$  fm emitting a gluon with energy  $\omega = 5$  GeV. The mass of the quark  $M = 4.75$  GeV. The DGLV opacity series calculated up to  $n=1$  (black), 3 (blue), 5 (green), 7 (orange), 9 (red) are shown in the figure. The opacity expansion computed up to ninth order is shown to converge to the ASW multiple soft scattering limit (maroon, dashed) for small  $k_{\perp} \lesssim \hat{q}L \approx 1$  GeV. At large  $k_{\perp}$ , differs from the ASW limit, DGLV has a robust Landau tail. Other parameters used in the simulation are:  $\lambda = 1.16$  fm,  $\mu = 0.5$  GeV,  $m_g = 0.356$  GeV,  $T = 0.258$  GeV,  $n_f = 0$ ,  $\alpha_s = 0.3$ .

# Running Coupling Effect 1

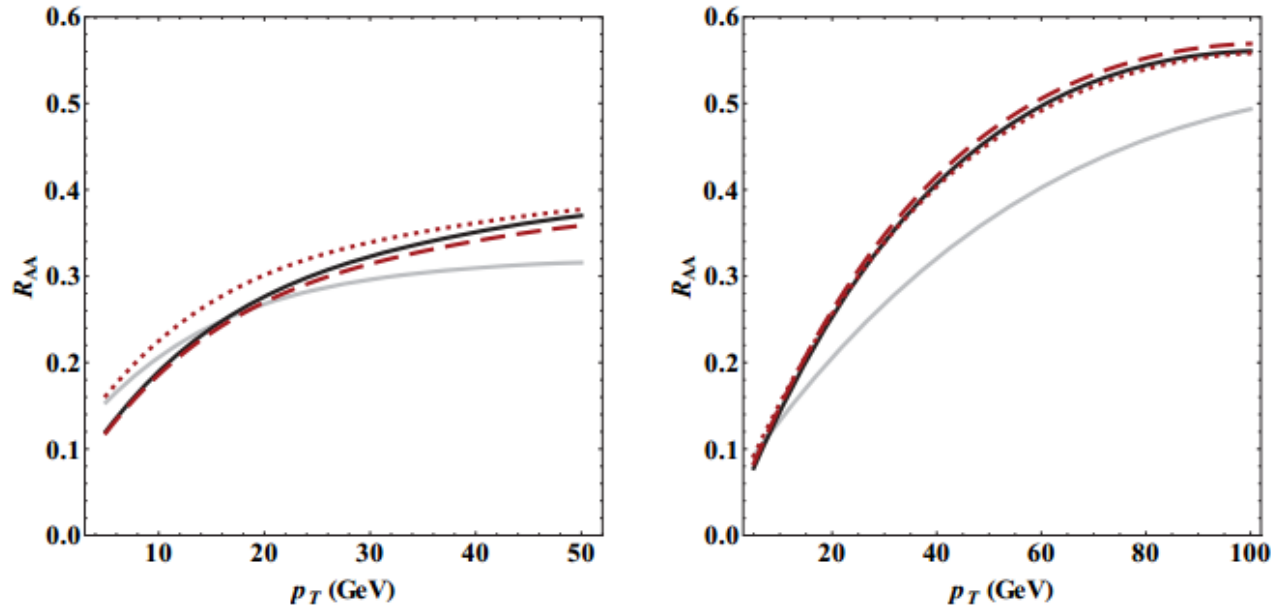


**Figure 1.** Fixed and running coupling pion  $R_{AA}$  results are compared side to side at RHIC (*left*) and LHC (*right*) in CUJET with Glauber static transverse plus Bjorken longitudinal expanding background. The gray opaque curves use a fixed coupling with  $\alpha_s = 0.3$ , while the black curves use a running coupling with  $\alpha_{max} = 0.4$ . The difference is notable, especially in the higher energy range available at the LHC, while RHIC results are left almost unchanged. The sensitivity to the variation of running scales  $Q_i$  (cf. Eq. (2.1) and following) is measured by the red curves: on one side we decrease the value of all scales  $Q_i$  by 50% and lower  $\alpha_{max}$  to 0.3 (red dashed), on the other we increase all scales  $Q_i$  by 25% and increase at the same time  $\alpha_{max}$  to 0.6 (red dotted).  $\alpha_{max}$  is constrained to fit  $R_{AA}^{\pi,LHC}(p_T \approx 30 \text{ GeV}) = 0.35$ .

## Running Coupling Effect 2

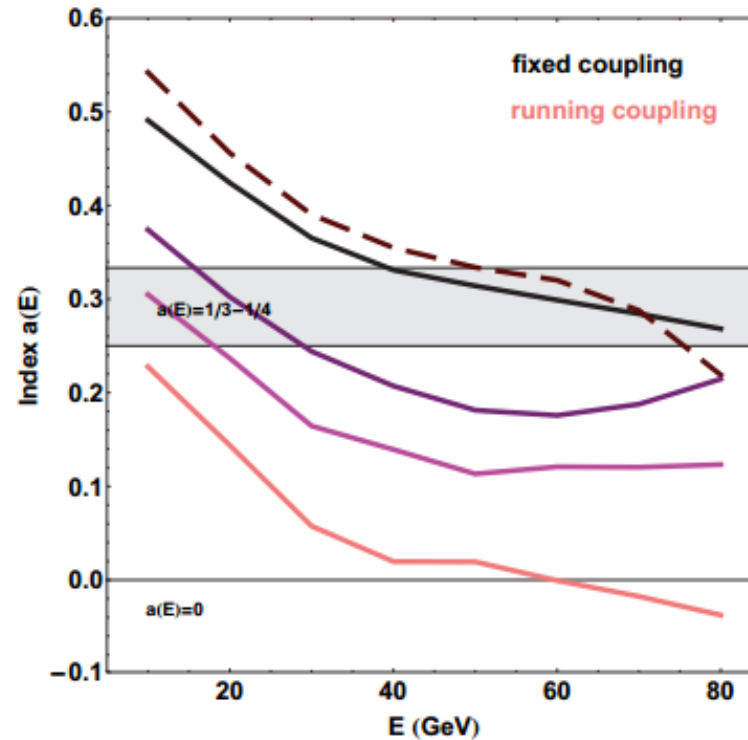


**Figure 2.** Energy loss index  $a(E)$  (cf. Eq. (2.9)) for different assumptions of the running coupling in CUJET: fixed effective  $\alpha_s = 0.3$  (black), only thermal coupling running (dashed red), only  $\alpha_s^2(\mathbf{q}^2)$  running (purple), only  $\alpha_s^2(\mathbf{k}^2/(x(1-x)))$  running (magenta), all couplings running (pink). The saturated  $\alpha_{max}$  value is chosen to be equal to 0.4, which corresponds to approximately  $Q_0 \sim 1$  GeV. The plot shows the energy loss of a light quark ( $M = 0.2$  GeV) traveling from the origin of the transverse plane and through a gluonic plasma ( $n_f = 0$ ) of size  $L = 5$  fm, whose density profile is generated from Glauber model and resembles the medium created in a Pb+Pb  $\sqrt{s_{NN}} = 2.76$  TeV  $b = 0$  fm collision.

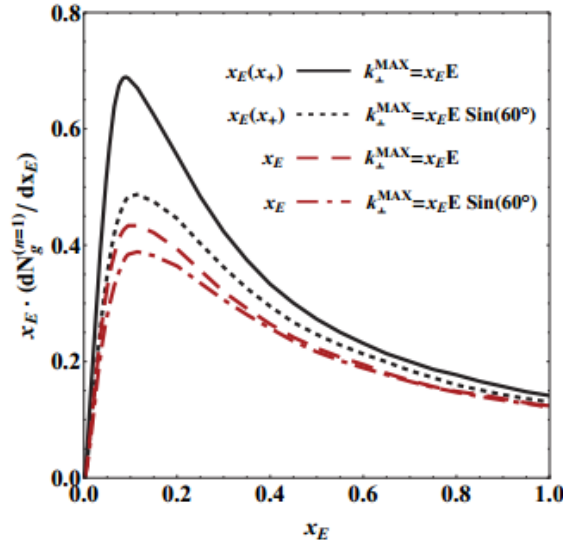


**Figure 16.**  $k_{\perp}$  integrated,  $n = 1$  gluon number distribution generated by a  $E = 20$  GeV light quark ( $M = 0.2$  GeV) jet traversing a brick plasma of thickness  $L = 5$  fm. The two interpretations of  $x$  as gluon fractional energy ( $x_E$ ) or gluon fractional plus-momentum ( $x_+$ ) lead to remarkably different results, especially in the soft  $x \ll 1$  region. The uncertainty due to the choice of  $\theta^{MAX}$  is noticeable but less prominent. Other parameters used in the simulation are:  $\lambda = 1.16$  fm,  $\mu = 0.5$  GeV,  $m_q = 0.356$  GeV,  $T = 0.258$  GeV,  $n_f = 0$ ,  $\alpha_s = 0.3$ .

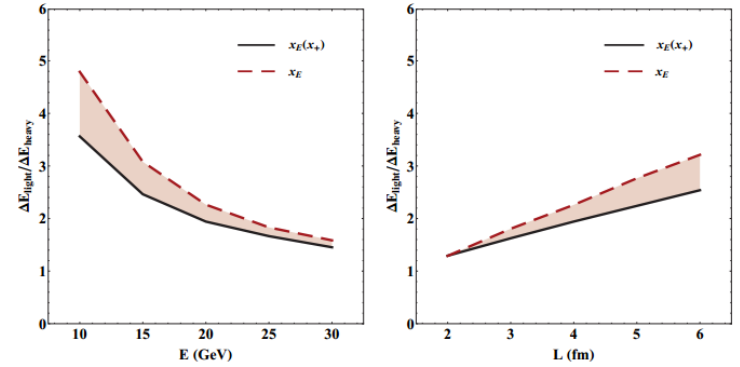
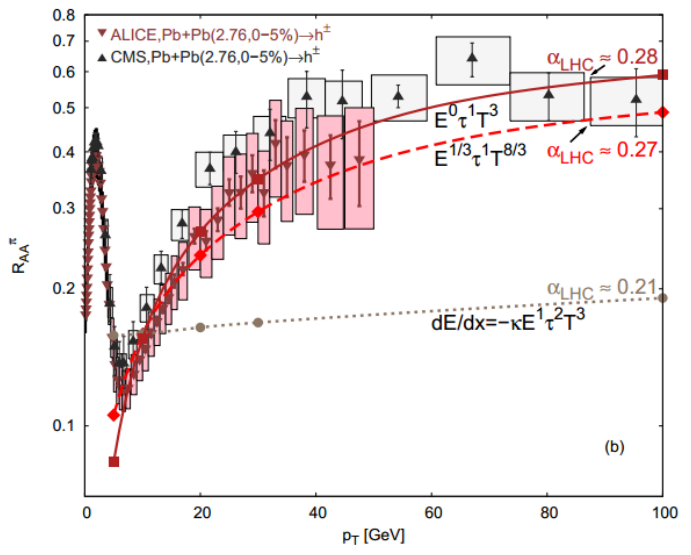
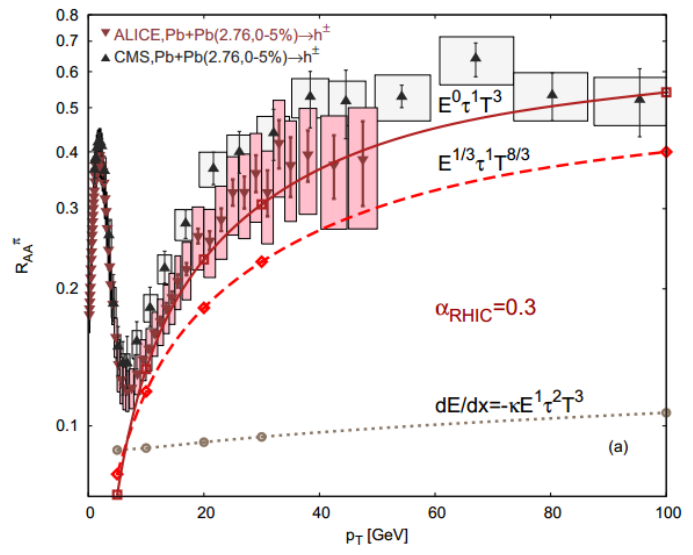
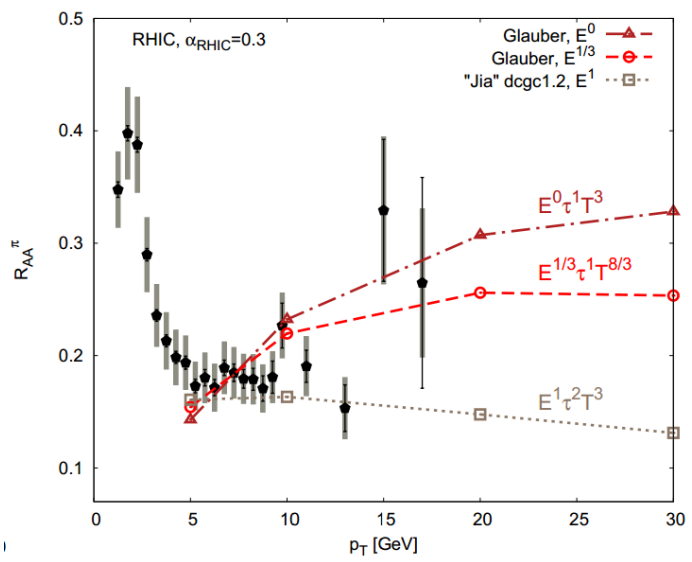
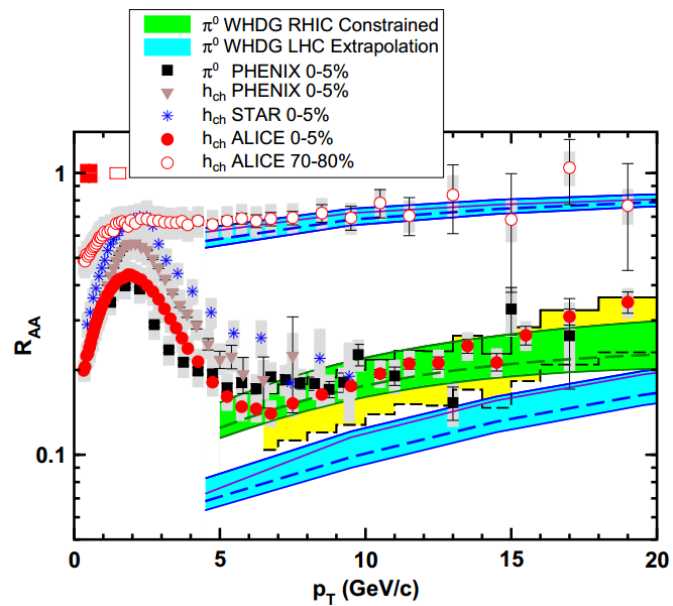


**Figure 17.** Energy loss ratio between light ( $M_l = 0.2$  GeV) and heavy quark ( $M_b = 4.75$  GeV) jets in a brick, for different interpretations of  $x$  as in Fig. 16. Here  $\alpha_s = 0.3$ ,  $L = 5$  fm (left),  $E = 20$  GeV (right) and the energy loss has been computed at first order  $n = 1$  in opacity. An error of approximately  $\sim 25\%$  is introduced for sufficiently small energies and large plasma sizes. Other parameters used in the simulation are:  $\lambda = 1.16$  fm,  $\mu = 0.5$  GeV,  $m_q = 0.356$  GeV,  $T = 0.258$  GeV,  $n_f = 0$ .

*Cf. also W. Horowitz and B. Cole (2010)*

# The surprising transparency of $sQGP$ at LHC



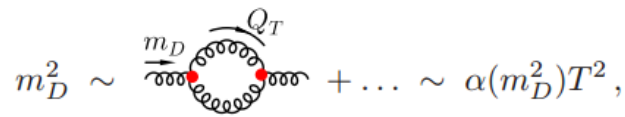
➤ Weaker than linear density dependence of jet opacity on the density NPA872,265(2011), PRC86,024903(2012)

# Questioning: scales in thermal coupling

❖ Peshier, arXiv:hep-ph/0601119 & Djordjevic and Djordjevic, arXiv:1307.4098

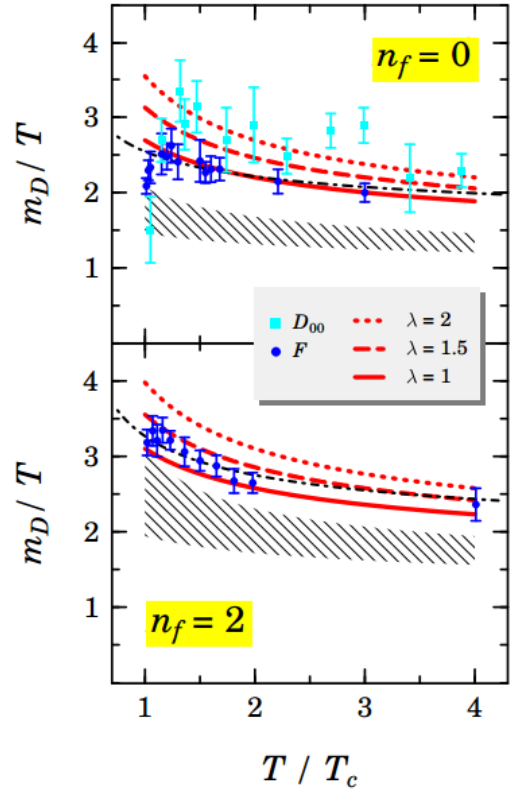
$$m_D^2 = \frac{1}{3} N_c \left(1 + \frac{1}{6} n_f\right) 4\pi\alpha(m_D^2) T^2 \quad \color{red}{=} \quad \frac{\mu_E^2}{\Lambda_{QCD}^2} \ln\left(\frac{\mu_E^2}{\Lambda_{QCD}^2}\right) = \frac{1 + n_f/6}{11 - 2/3 n_f} \left(\frac{4\pi T}{\Lambda_{QCD}}\right)^2$$

“ be related to a specific quantity/scale. The correct scale, which should be an outcome of the calculation rather than ‘chosen’, is crucial in particular for larger coupling. The relevant scale for the Debye mass, ”



is  $m_D$  itself, not the typical loop momentum  $Q_T \sim 2\pi T$  as often presumed. It's the interplay between vacuum and thermal fluctuations (accounted for by renormalization) that leads to the implicit Eq. (7), which is manifestly finite and gauge and renormalization group invariant. The soft(er) scale in the coupling,  $m_D \sim \sqrt{\alpha} T \ll T$  for  $\alpha \ll 1$ , yields stronger screening than previously estimated from (1). Remarkably, both the novel result

Peshier, arXiv:hep-ph/0601119



# Dynamical (non-Thermal) Radiative Running Coupling(s)

❖ Horowitz and Kovchegov, Nucl. Phys. A849, 72 (2011)

“

ABSTRACT: We calculate running coupling corrections for the lowest-order gluon production cross section in high energy hadronic and nuclear scattering using the BLM scale-setting prescription. In the final answer for the cross section the three powers of fixed coupling are replaced by seven factors of running coupling, five in the numerator and two in the denominator, forming a ‘septumvirate’ of running couplings, analogous to the ‘triumvirate’ of running couplings found earlier for the small- $x$  BFKL/BK/JIMWLK evolution equations. It is interesting to note that the two running couplings

To include running coupling corrections we will follow the BLM scale-setting procedure [54]. We will first resum the contribution of all quark bubble corrections giving powers of  $\alpha_\mu N_f$ , with  $N_f$  the number of quark flavors and  $\alpha_\mu$  the physical coupling at some arbitrary renormalization scale  $\mu$ . We will then complete  $N_f$  to the full beta-function by replacing

$$N_f \rightarrow -6 \pi \beta_2 \quad (3.1)$$

in the obtained expression. Here

$$\beta_2 = \frac{11N_c - 2N_f}{12 \pi} \quad (3.2)$$

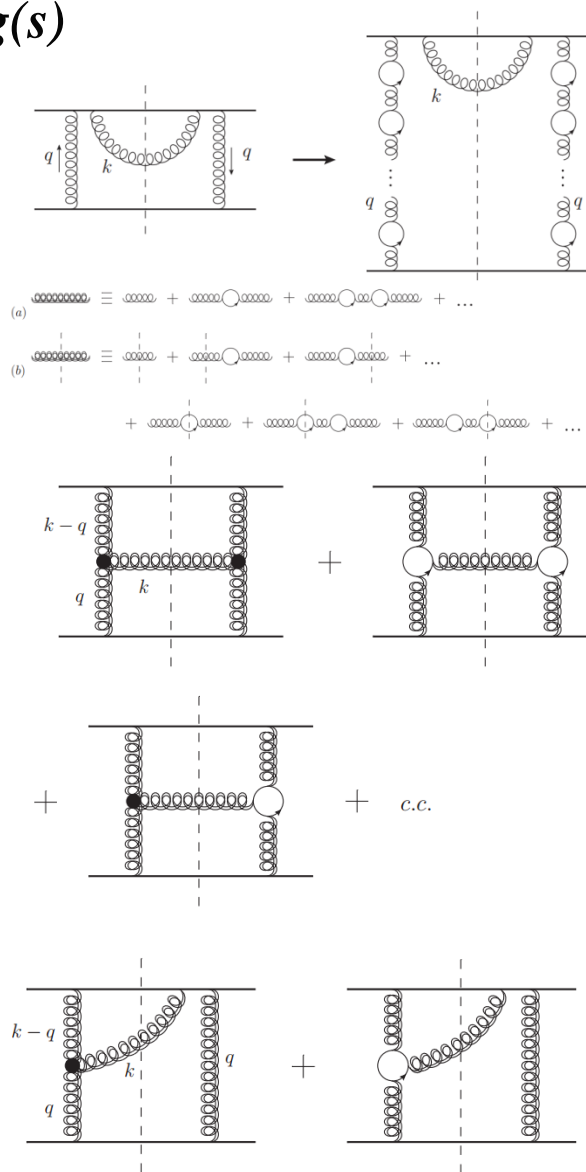
is the one-loop QCD beta-function. After this, the powers of  $\alpha_\mu \beta_2$  should combine into physical running couplings

$$\alpha_s(Q^2) = \frac{\alpha_\mu}{1 + \alpha_\mu \beta_2 \ln \frac{Q^2}{\mu^2}} \quad (3.3)$$

$$\frac{d\sigma}{d^2k_T dy} = \frac{2 C_F}{\pi^2} \frac{\alpha_s (\Lambda_{\text{coll}}^2 e^{-5/3})}{\mathbf{k}^2} \int \frac{d^2q}{q^2 (\mathbf{k}-\mathbf{q})^2} \frac{\alpha_s^2 (q^2 e^{-5/3})}{\alpha_s(Q^2 e^{-5/3})} \frac{\alpha_s^2 ((\mathbf{k}-\mathbf{q})^2 e^{-5/3})}{\alpha_s(Q^* e^{-5/3})} \quad (3.31)$$

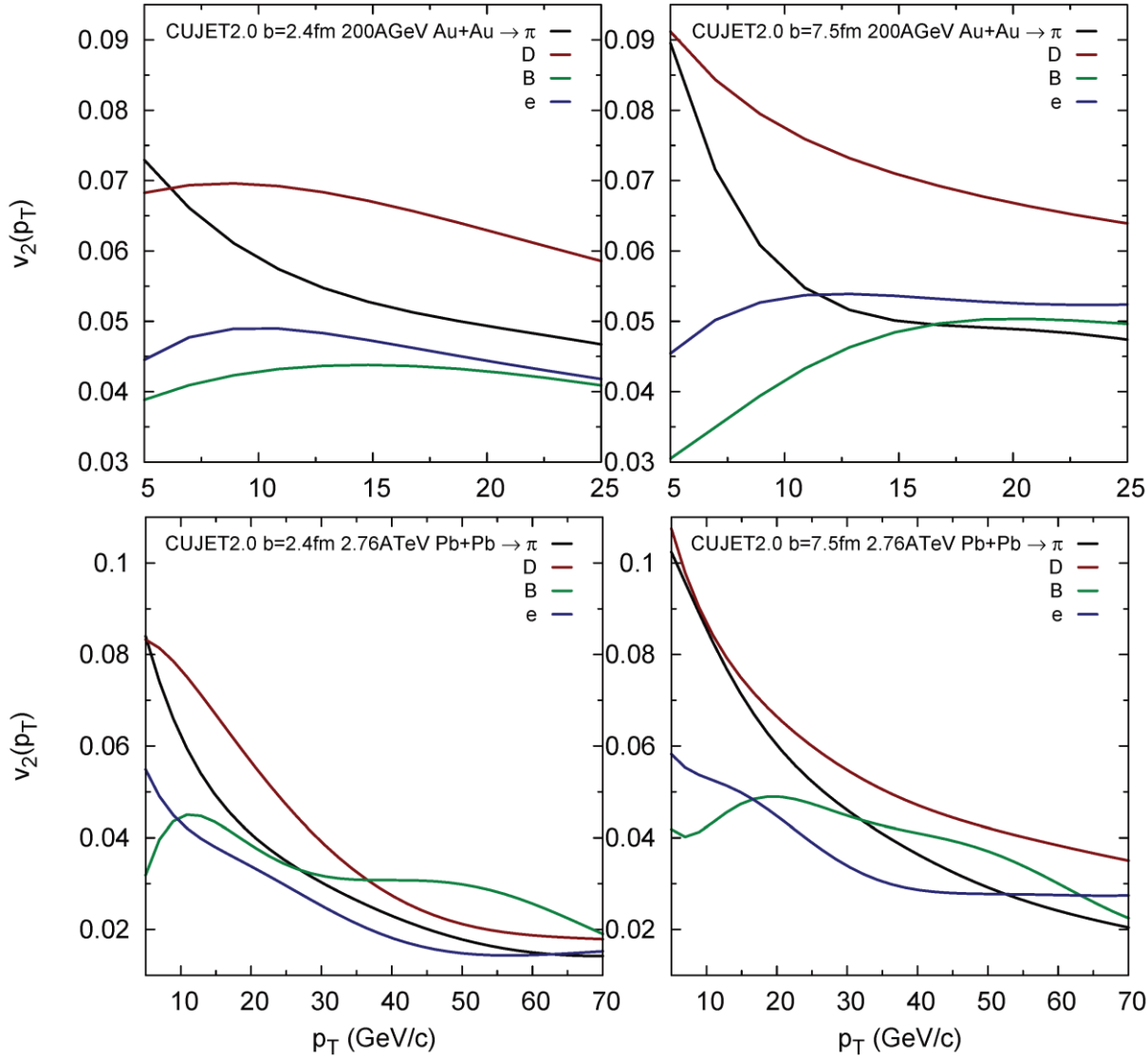
with the  $\mu_{\text{MS}}$ -independent momentum scale  $Q$  defined by

$$\begin{aligned} \ln \frac{Q^2}{\mu_{\text{MS}}^2} &= \frac{1}{2} \ln \frac{q^2 (\mathbf{k}-\mathbf{q})^2}{\mu_{\text{MS}}^4} - \frac{1}{4 q^2 (\mathbf{k}-\mathbf{q})^2 [( \mathbf{k}-\mathbf{q})^2 - q^2]^6} \left\{ \mathbf{k}^2 [(\mathbf{k}-\mathbf{q})^2 - q^2]^3 \right. \\ &\times \left\{ [(\mathbf{k}-\mathbf{q})^2]^2 - (q^2)^2 \right\} [(\mathbf{k}^2)^2 + ((\mathbf{k}-\mathbf{q})^2 - q^2)^2] + 2 \mathbf{k}^2 [(q^2)^3 - [(\mathbf{k}-\mathbf{q})^2]^3] \\ &- q^2 (\mathbf{k}-\mathbf{q})^2 [2 (\mathbf{k}^2)^2 + 3 [(\mathbf{k}-\mathbf{q})^2 - q^2]^2 - 3 \mathbf{k}^2 [(\mathbf{k}-\mathbf{q})^2 + q^2]] \ln \left( \frac{(\mathbf{k}-\mathbf{q})^2}{q^2} \right) \left. \right\} \\ &+ i [(\mathbf{k}-\mathbf{q})^2 - q^2]^3 \left\{ \mathbf{k}^2 [(\mathbf{k}-\mathbf{q})^2 - q^2] [\mathbf{k}^2 [(\mathbf{k}-\mathbf{q})^2 + q^2] - (q^2)^2 - [(\mathbf{k}-\mathbf{q})^2]^2] \right. \\ &+ q^2 (\mathbf{k}-\mathbf{q})^2 \left( \mathbf{k}^2 [(\mathbf{k}-\mathbf{q})^2 + q^2] - 2 (\mathbf{k}^2)^2 - 2 [(\mathbf{k}-\mathbf{q})^2 - q^2]^2 \right) \ln \left( \frac{(\mathbf{k}-\mathbf{q})^2}{q^2} \right) \left. \right\} \\ &\times \sqrt{2 q^2 (\mathbf{k}-\mathbf{q})^2 + 2 \mathbf{k}^2 (\mathbf{k}-\mathbf{q})^2 + 2 q^2 \mathbf{k}^2 - (\mathbf{k}^2)^2 - (q^2)^2 - [(\mathbf{k}-\mathbf{q})^2]^2} \left. \right\}. \quad (3.32) \end{aligned}$$



$$\int \frac{d^4k}{(2\pi)^4} = \int_{-\infty}^{\infty} dk^2 \int \frac{dk^+ d^2k_\perp}{2k^+ (2\pi)^4} \Rightarrow \int_0^{\Lambda_{\text{coll}}^2} dk^2 \int \frac{dk^+ d^2k_\perp}{2k^+ (2\pi)^4}$$

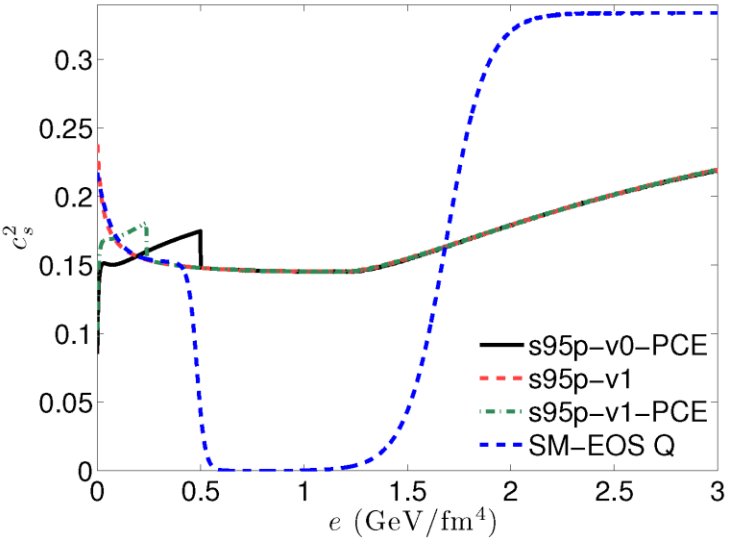
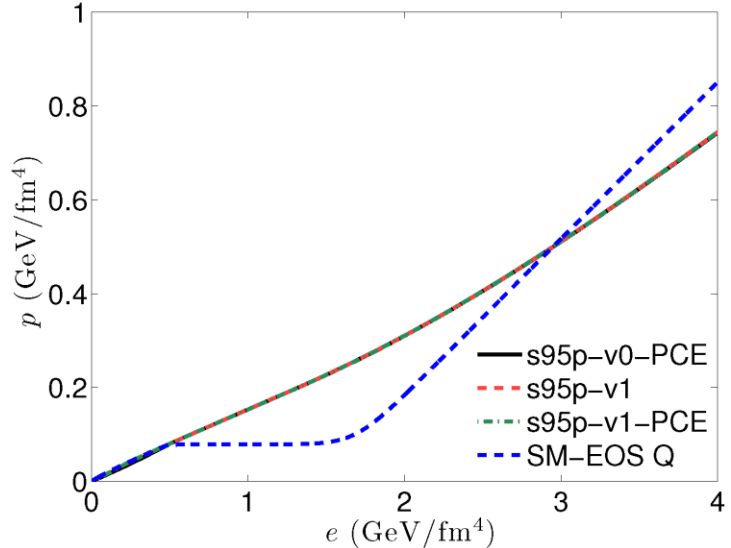
# CUJET2.0 Result: flavor $v_2$



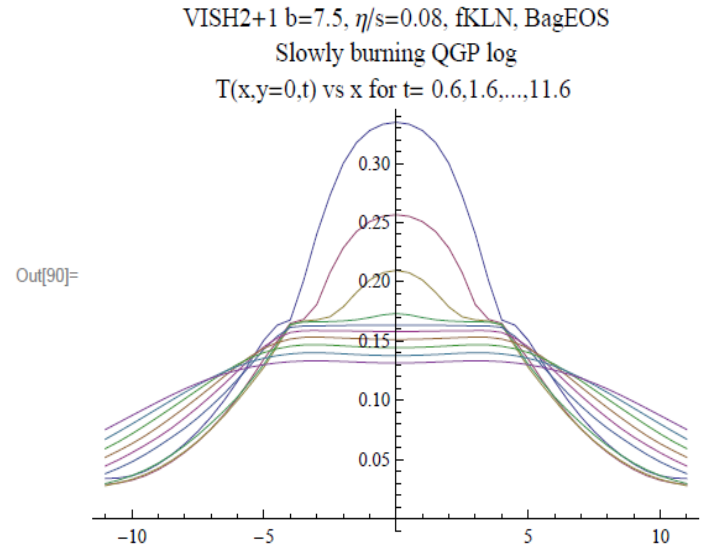
- ❖ B meson  $v_2$  has a peak at  $p_T \sim 10\text{GeV}$  @  $b=2.4\text{fm}$  and  $p_T \sim 20\text{GeV}$  @  $b=7.5\text{fm}$  at both RHIC and LHC
- ❖ Semi-ordering of the position of the peak for different flavor  $v_2$



# VISH2+1 More on EOS

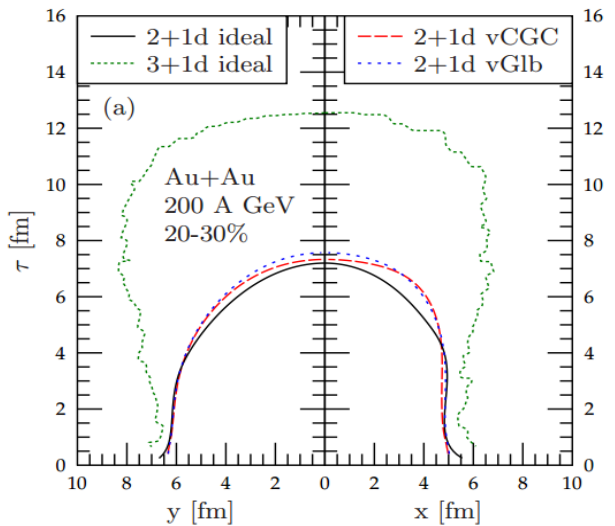


■ VISH2 + 1 with  $\eta = 0.08$  ideal fluid results for RHIC  $b = 7$  fm

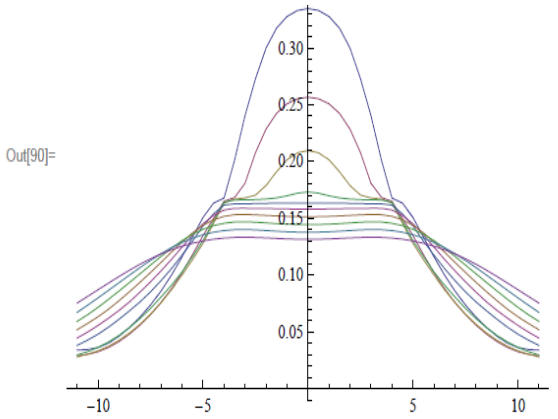


T. Renk, H. Holopainen, U. Heinz and C. Shen, PRC 83, 014910 (2011)  
 C. Shen, U. Heinz, P. Huovinen and H. Song, PRC 82, 054904 (2010)  
 H. Song and U. Heinz, PRC 78, 024902 (2008)

# CUJET2.0 = rcDGLV + Elastic + 2+1D Viscous Hydro



T. Renk, H. Holopainen, U. Heinz and C. Shen, PRC 83, 014910 (2011)  
 C. Shen, U. Heinz, P. Huovinen and H. Song, PRC 82, 054904 (2010)  
 H. Song and U. Heinz, PRC 78, 024902 (2008)



- ❖ Couple rcDGLV to VISH 2+1D expanding QGP fluid fields ( $T(x,t), v(x,t)$ )
- ❖ RHIC Au+Au 200AGeV
  - Equation of State: s95p-PCE
  - Initial Condition: MC-Glauber
  - $\eta/s=0.08$
  - Initial Time: 0.6fm/c
  - Cooper-Frye freeze-out temperature: 120MeV
- ❖ LHC Pb+Pb 2.76ATeV
  - Equation of State: s95p-PCE
  - Initial Condition: MC-Glauber
  - $\eta/s=0.08$
  - Initial Time: 0.6fm/c
  - Cooper-Frye freeze-out temperature: 120MeV
- ❖ Compatible with measurements of low pT particle production spectra and flow harmonics